

THE DEVELOPMENT OF THE CHARACTERISTIC GRID FOR SUPERSONIC  
DIVERGING JETS EXHAUSTING INTO A HYPERSONIC  
PARALLEL FLOWING STREAM

by

CALVIN SCOTT HENRY

A THESIS

submitted to


OREGON STATE COLLEGE

in partial fulfillment of  
the requirements for the  
degree of


MASTER OF SCIENCE


June 1960


APPROVED:

  
\_\_\_\_\_  
Professor of Mechanical Engineering

In Charge of Major

  
\_\_\_\_\_  
Head of Mechanical Engineering Department

  
\_\_\_\_\_  
Chairman of School Graduate Committee

  
\_\_\_\_\_  
Dean of Graduate School

Date thesis is presented 12/4/59

Typed by Sharon Woodall

# TABLE OF CONTENTS

	Page
INTRODUCTION . . . . .	1
NOTATION . . . . .	4
THE METHOD OF CHARACTERISTICS . . . . .	7
THE LEADING MACH LINE. . . . .	10
DEVELOPMENT OF THE CHARACTERISTIC GRID . . . . .	16
Interior Points . . . . .	16
Corner Expansion Calculation. . . . .	21
Point Next to the Axis of Symmetry Calculation. . . . .	23
Point on the Axis of Symmetry Calculation . .	27
Leading Mach Line for Constant Area Nozzle Calculation. . . . .	31
CONSTRUCTION OF THE CHARACTERISTIC GRID. . . . .	34
COMPUTER CALCULATIONS. . . . .	39
Initial Programs. . . . .	39
Method of Calculation . . . . .	40
Initial Input . . . . .	40
Individual Calculation. . . . .	42
Program Conveniences. . . . .	44
Convergence Criteria. . . . .	46
CONCLUSIONS AND RECOMMENDATIONS. . . . .	49
BIBLIOGRAPHY . . . . .	51
APPENDIX . . . . .	53



## LIST OF FIGURES

Figure		Page
1.	Source Flow Nozzle	12
2.	Interior Point Calculation	17
3.	Point Next to the Axis of Symmetry Calculation	24
4.	Point on the Axis of Symmetry Calculation	28
5.	Constant Area Nozzle	32
6.	Characteristic Grid	35
7.	Point on the Leading Mach Line Program	55
8.	Corner Expansion Program	59
9.	Combined Program	65
10.	Constant Area Nozzle Program	78
11.	Tape Program	80



# THE DEVELOPMENT OF THE CHARACTERISTIC GRID FOR SUPERSONIC DIVERGING JETS EXHAUSTING INTO A PARALLEL HYPERSONIC FLOWING STREAM

## INTRODUCTION

In this age of rockets, missiles, and other supersonic vehicles, increasing interest has been associated with the use of jet propulsion systems. Probably the most predominant interest in underexpanded jets is the jet interference which may impinge on the missile structure in the neighborhood of the jet exit. The structure of the jet exhaust is also associated with the problems dealing with jet noise (5, p. 5).

This paper is intended to be an extension and generalization of a thesis already written on the same subject by John Newton (7). His paper, which was only concerned with constant area nozzles, concentrated on attaining the jet boundary rather than determining the jet flow field. His completed project required precalculated information about the flow field. Therefore, the project was not particularly interested in the internal flow properties. The problem under consideration in this paper is the determination of the internal flow properties not only for constant area nozzles, but for diverging nozzles also. Therefore, with the combined papers, the fluid properties and location of the jet boundary can be calculated independently of any precalculated information.

### Method of Solution

The solution of a supersonic inviscid jet flow field can be determined by applying the method of characteristics. The method of characteristics is a method of solving the characteristic equations which describe the supersonic flow. This method determines the properties in the interior of the jet flow field. The characteristic equations are solved numerically by programming them on the ALWAC-III E electronic digital computer.

### Scope of Thesis

A method of determining the jet flow properties of conically divergent nozzles exhausting into a uniform flowing hypersonic stream has been accomplished. The method of characteristics is used to solve the characteristic equations and establish the properties in the jet flow field. The method of developing the flow field, and some of the difficulties involved in doing so, is presented. The characteristic equations are programmed in finite difference form on the ALWAC-III E electronic digital computer. The computer programs for all the different type individual calculations involved are included and discussed.

### Assumptions

It is assumed throughout the paper that the fluid is a perfect gas having no viscosity and a constant specific heat at constant pressure. The flow of the jet is assumed to be axially symmetric, steady, supersonic, and irrotational. The flow is also isentropic, which is implied by the condition of irrotationality. It is also assumed that the exit flow of the diverging nozzle is conical.



## NOTATION

A	defined by equation 19
A'	defined by equation 19a
A''	defined by equation 19b
B	defined by equation 20
B'	defined by equation 20a
c	local speed of sound
c*	speed of sound at Mach Number of unity
C	defined by equation 21
C'	defined by equation 21a
C <sub>1</sub>	a constant
C <sub>2</sub>	a constant
C <sub>3</sub>	a constant
D	defined by equation 22
D'	defined by equation 22a
e	maximum number of points on the leading Mach line left to be calculated
E	maximum number of points to be calculated along leading characteristic line
E'	defined by equation 23
E''	defined by equation 23a
F	defined by equation 24
F'	defined by equation 24a
G	defined by equation 34
H	defined by equation 35
I	defined by equation 42

J	$ \Delta\alpha  - \epsilon$
k	ratio of specific heats
l	$ \Delta\theta  - \epsilon$
l	distance from lip of constant area nozzle to point under consideration on leading characteristic line
M	dimensionless velocity $V/c$ known as Mach Number
M*	dimensionless velocity $V/c^*$
n	number of points on axis of symmetry left to be calculated
n	distance from source point to point on leading characteristic line
n'	number of points on axis of symmetry to be calculated
o'	$ \Delta M^*  - \epsilon$
P	pressure
r	number of interior points left to be calculated
t	defined by equation 12
V	total velocity
V*	total velocity at Mach Number of unity
x	axial coordinate
y	radial coordinate
$\theta$	included angle between velocity vector and x-axis
$\phi$	velocity potential
$\alpha$	Mach angle
$\rho$	density
$\rho^*$	density at Mach Number of unity
$\epsilon$	convergence limit

- $\Delta$  denotes the change in
- ( )<sub>I</sub> denotes right running characteristic family I
- ( )<sub>II</sub> denotes left running characteristic family II
- ( )<sub>b</sub> denotes jet boundary condition
- ( )<sub>e</sub> denotes nozzle exit condition
- ( )<sub>n</sub> denotes values at nozzle wall
- ( )<sub>j</sub> denotes jet flow field condition
- ( )<sub>x</sub> denotes value at point under consideration
- ( ) <sub>$\infty$</sub>  denotes exterior flow field



# THE METHOD OF CHARACTERISTICS

The motion of a supersonic stream can be described by a system of second order partial differential equations of the hyperbolic type. Each solution to the differential equations represents a three dimensional surface in  $x$ ,  $y$ , and  $\phi$  space. It is possible that curves exist in these surfaces which represent the location of discontinuities in some of the derivatives of the fluid properties. These curves, if they do exist, are called the characteristic curves of the solution. Therefore, characteristic curves exist when the transition from one region of the flow field to another involves a discontinuity in some of the derivatives (9, p. 584). The projections of the three dimensional characteristic lines on the  $x$ ,  $y$  plane are called the physical characteristics, and the projections on the  $\theta$ ,  $V$  plane are called the hodograph characteristics.

An examination of the potential equation for possible discontinuities in the derivatives of the fluid properties results in the following equations for axially symmetric, supersonic, irrotational, steady flow (10, p. 677).

$$\frac{(dy)}{(dx)_{I,II}} = \tan(\theta + \alpha) \quad (1)$$

and

$$(d\theta)_{I,II} = \mp \frac{\cot \alpha}{M^2} (dM^2)_{I,II} + \frac{\sin \theta \sin \alpha}{y \sin(\theta + \alpha)} (dy)_{I,II} \quad (2)$$

These differential equations are the characteristic equations of the solution for the flow field.

In the above two equations, the upper sign refers to the right running characteristic family I, which forms an angle of  $(\theta - \alpha)$  with the positive x axis in the physical plane. The lower sign refers to the left running characteristic family II, which forms an angle of  $(\theta + \alpha)$  with the positive x axis in the physical plane. In looking down the velocity vector in the direction of the flow, the characteristic lines of family I turn off to the right while the characteristic lines of family II turn off to the left (3, p. 10). Equation 1 represents the characteristic solution in the physical plane, and equation 2 represents the characteristic solution in the hodograph plane.

An examination of equations 1 and 2 reveals that the characteristic equations for axially symmetric flow are dependent on both the physical and hodograph planes. Therefore, the solution of the flow field must be constructed simultaneously in both the physical and hodograph planes (10, p. 678). The fluid properties of the flow field for axially symmetric flow are a function of the velocity. Therefore, once the velocity vector pattern of the flow field is known, all the fluid properties of the flow field are also known.

The equations of the characteristic lines in the physical and hodograph planes are expanded into a finite difference form for actual calculations. The intersection points of the two families of characteristics are connected by straight line segments. The line segments are used to approximate the system of continuous characteristic curves. The accuracy of this method depends on the accuracy of the input data, the size of the grid developed and the degree of convergence used in the calculations (9, p. 619).



## LEADING MACH LINE

The diverging nozzle under consideration was assumed to give conical exit flow. Conical flow is a flow in which all the fluid properties are uniform on rays passing through a common vertex (11, p. 729). In the case of a supersonic diverging nozzle, the flow would have to originate from a point to produce a conical exit flow. Although this type of a nozzle is a simplification, it is representative of nozzles used to produce supersonic flow and will serve as a good basis for the study of underexpanded jets.

An examination of the potential equation for conical supersonic flow reveals that a pure source flow is a possible solution (9, p. 237). By representing the flow in the conical nozzle with a source flow, points along the leading characteristic line can be readily calculated. The leading characteristic line represents the first disturbance that is felt by the flow in the nozzle due to the sharp corner at the exit of the nozzle. Points on the leading characteristic line represent the input data for the development of the characteristic grid. The local Mach line and the characteristic line are one and the same.

The properties calculated for each point in the characteristic grid are  $x$ ,  $y$ ,  $M^*$ ,  $M$ ,  $\theta$ , and  $\alpha$ . These properties are sufficient to fully describe the entire

flow field.

Consider a conically divergent nozzle assumed to give pure source flow with the coordinates as shown in figure 1 (4, p. 25). Polar coordinates,  $N$  and  $\theta$ , are used with the origin at the source point. The angle  $\theta$  is measured counter clockwise from the axis of symmetry. From figure 1 the rectangular coordinates for points on the leading Mach line are as follows.

$$Y = N \sin \theta \quad (3)$$

and

$$X = N \cos \theta - N_n \cos \theta_n \quad (4)$$

The characteristic equation in the hodograph plane for a supersonic source flow such as this is equation 2. The following notation was used to simplify the characteristic equation in the hodograph plane.

$$dt = \pm \frac{\cot \alpha}{M^*} (dM^*)_{I,II} \quad (5)$$

By substituting this relation into equation 2, the result is

$$d(\theta \pm t)_{I,II} = \pm \frac{\sin \theta \sin \alpha}{y \sin(\theta \mp \alpha)} (dy)_{I,II} \quad (2a)$$

In the case of the leading characteristic line, which represents a right running characteristic line, equation 5 becomes

$$dt = \frac{\cot \alpha}{M^*} dM^* \quad (5a)$$

# SOURCE FLOW NOZZLE

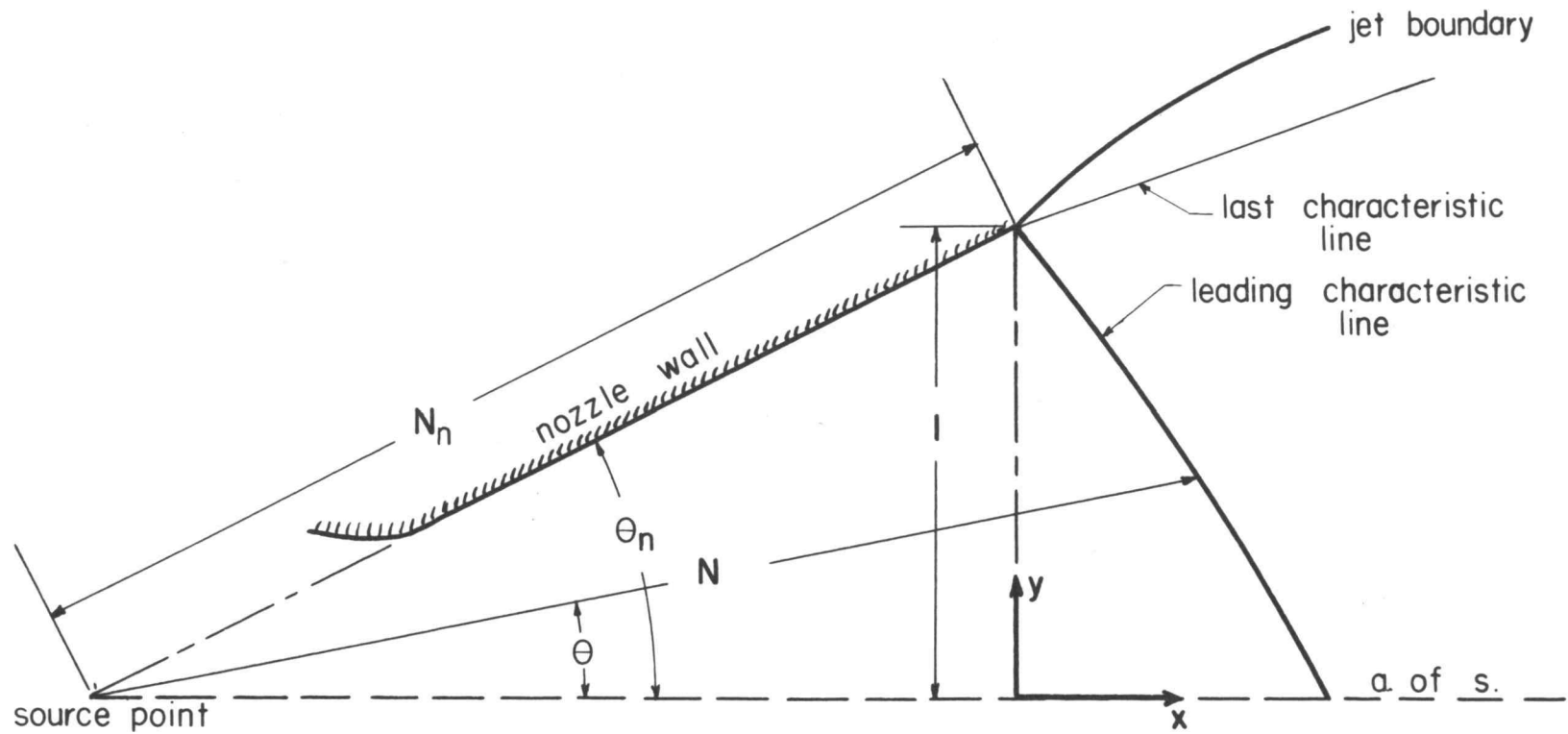


FIGURE I



For isentropic flow

$$M^* = \left\{ \frac{\frac{k+1}{2} M^2}{1 + \frac{k-1}{2} M^2} \right\}^{\frac{1}{2}} \quad (6)$$

By taking the derivative of equation 6, the result is

$$dM^* = \frac{\frac{k+1}{2} M dM}{M^* \left[ 1 + \frac{k-1}{2} M^2 \right]^{\frac{3}{2}}} \quad (7)$$

Combining equations 6 and 7 yields

$$\frac{dM^*}{M^*} = \frac{dM}{M \left( 1 + \frac{k-1}{2} M^2 \right)} \quad (8)$$

The Mach angle,  $\alpha$ , is defined by the relation

$$\alpha = \tan^{-1} \left\{ \frac{1}{\sqrt{M^2 - 1}} \right\} \quad (9)$$

By solving equation 9 for M, the result is

$$M = \operatorname{cosec} \alpha \quad (10)$$

The derivative of equation 10 is

$$dM = -\cot \alpha \operatorname{cosec} \alpha d\alpha \quad (11)$$

Combining equations 8, 11 and 5a results in the following expression for dt.

$$dt = - \frac{\cot^2 \alpha d\alpha}{1 + \frac{k-1}{2} \operatorname{cosec}^2 \alpha} \quad (5b)$$

When equation 5b is integrated for the case of the leading characteristic line, it yields

$$t = \alpha + \sqrt{\frac{k+1}{k-1}} \cot^{-1} \left\{ \sqrt{\frac{k+1}{k-1}} \tan \alpha \right\} - \frac{\pi}{2} \quad (12)$$

Along Mach lines, the following equation is true (4, p. 27).

$$(2\theta \pm t)_{I,II} = C_1 \quad (13)$$

The negative sign can be excluded since the leading characteristic (Mach) line represents a line of the right running characteristic family.

Equation 13 then becomes

$$2\theta + t = C_1 \quad (13a)$$

From the equation of continuity for a pure source flow (4, p. 26).

$$N^2 = \frac{C_2}{V\rho} \quad (14)$$

For adiabatic flow

$$\frac{\rho V}{\rho^* V^*} = \left\{ \frac{k+1}{2} \right\}^{2(k-1)} \left[ \frac{M}{\left\{ \frac{k-1}{2} M^2 + 1 \right\}^{\frac{k+1}{2(k-1)}}} \right] \quad (15)$$

Therefore, by combining equations 14 and 15

$$N^2 = C_2' \frac{\left[ \frac{k-1}{2} M^2 + 1 \right]^{\frac{k+1}{2(k-1)}}}{M} \quad (16)$$

Now, from equation 10

$$M = \frac{1}{\sin \alpha} \quad (10a)$$

Combining the two equations, 10a and 16, and solving for

N results in

$$N = C_2' \left[ 1 + \frac{2}{k+1} \sin^2 \alpha \right]^{\frac{k+1}{4(k-1)}} (\sin \alpha)^{-\frac{1}{k-1}} \quad (17)$$

By substituting equation 12 into equation 13a, and solving for  $\theta$ , the result is

$$\theta = \frac{C_1 - \alpha \left( \frac{k+1}{k-1} \right)^{\frac{1}{2}} \cot^{-1} \left[ \left( \frac{k+1}{k-1} \right)^{\frac{1}{2}} \tan \alpha \right] + \frac{\pi}{2}}{2} \quad (18)$$

The constants  $C_1$  and  $C_2'$  can be found from the boundary conditions at the sharp corner of the nozzle. The value of  $N$  at this point is  $N_n$ . The Mach number at the lip is specified in any given problem; therefore, so is  $\alpha$  since  $\alpha$  is a function of the Mach number only. With these two properties known, it is possible to solve equation 17 for  $C_2'$ . The value of  $\theta$  at the lip of the nozzle is  $\theta_n$ . Therefore, equation 1 can be solved for  $C_1$ .

With these equations and the initial conditions at the nozzle lip just prior to exit, the flow properties and the Cartesian coordinates of points along the leading characteristic line, or Mach line, can be determined. These points can be considered the initial input for the development of the characteristic grid.

## DEVELOPMENT OF THE CHARACTERISTIC GRID

The points and all their fluid properties have been determined along the leading characteristic line and represent input data for the development of the characteristic grid. The development of the characteristic grid involved three different types of calculations, and each was examined in detail. The different calculations are encountered when boundary conditions are imposed on the characteristic equations (9, p. 620). Due to the symmetry of the problem, the solution of the flow field for the upper half of the  $x, y$  plane is sufficient for the solution of the entire flow field.

### Interior Points

An interior point and all its fluid properties are found from the intersection of a right running characteristic line and a left running characteristic line. These points are always found in the interior of the flow and involve no boundary conditions. The notation and physical concept for the determination of an interior point is shown in figure 2. All the properties of points 1 and 2 are known. Point 3' represents the intersection of the right running characteristic line 1-3 with the left running characteristic line 2-3. Since point 3' is a solution of the two characteristic families, it is described by

17



equations 1 and 2.

1. First Approximation. The following notations are used to simplify the characteristic equations.

$$A = \tan (\theta_1 - \alpha_1) \quad (19)$$

$$B = \tan (\theta_2 + \alpha_2) \quad (20)$$

$$C = \frac{\cot \alpha_1}{M_1^*} \quad (21)$$

$$D = \frac{\cot \alpha_2}{M_2^*} \quad (22)$$

$$E' = \frac{\sin \theta_1 \sin \alpha_1}{y_1 \cos (\theta_1 - \alpha_1)} \quad (23)$$

$$F = \frac{\sin \theta_2 \sin \alpha_2}{y_2 \cos (\theta_2 + \alpha_2)} \quad (24)$$

The characteristic equations in finite difference form for the chord 1-3, which represents a right running characteristic line, are

$$y_3 - y_1 = A (x_3 - x_1) \quad (25)$$

for the physical plane, and

$$\theta_3 - \theta_1 = -C (M_3^* - M_1^*) + E' (x_3 - x_1) \quad (26)$$

for the hodograph plane. The corresponding characteristic equations for the chord 2-3, which represents a left running characteristic line, are

$$y_3 - y_2 = B (x_3 - x_2) \quad (27)$$

for the physical plane, and

$$\theta_3 - \theta_2 = D (M_3^* - M_2^*) - F (x_3 - x_2) \quad (28)$$

for the hodograph plane. The form of the hodograph equations for both characteristic lines have been changed slightly from equation 2 by substituting for the differential term  $dy$  from equation 1. By doing this, the possibility of dividing by zero when  $\theta$  is equal to  $\alpha$  is eliminated.

Equations 25 and 27 are solved simultaneously for  $x_3$  and  $y_3$ . These values are then used in equations 26 and 28 which are then solved simultaneously for  $M_3^*$  and  $\theta_3$ . This first procedure of finding the properties of point 3 assumed that the coefficients of the differentials for the characteristic line 1-3 had the properties of point 1, and the coefficients of the differentials for the characteristic line 2-3 had the properties of point 2. Therefore, the first evaluation of point 3 is termed the first approximation and involves some degree of error.

2. Successive Iterations. The approximate results already found may be improved by a rapidly convergent iteration procedure which rests on the use of average conditions between 1-3 and 2-3 (9, p. 619). Since tentative values of the properties for point 3 have already been found, the entire computation is repeated using the average coefficients along the chords 1-3 and 2-3. Using this procedure, the coefficients become

$$A' = \frac{1}{2} \left[ \tan (\theta_1 - \alpha_1) + \tan (\theta_3 - \alpha_3) \right] \quad (19a)$$

$$B' = \frac{1}{2} \left[ \tan (\theta_2 + \alpha_2) + \tan (\theta_3 + \alpha_3) \right] \quad (20a)$$

$$C' = \frac{1}{2} \left[ \frac{\cot \alpha_1}{M_1^*} + \frac{\cot \alpha_3}{M_3^*} \right] \quad (21a)$$

$$D' = \frac{1}{2} \left[ \frac{\cot \alpha_2}{M_2^*} + \frac{\cot \alpha_3}{M_3^*} \right] \quad (22a)$$

$$E'' = \frac{1}{2} \left[ \frac{\sin \theta_1 \sin \alpha_1}{y_1 \cos (\theta_1 - \alpha_1)} + \frac{\sin \theta_3 \sin \alpha_3}{y_3 \cos (\theta_3 - \alpha_3)} \right] \quad (23a)$$

$$F' = \frac{1}{2} \left[ \frac{\sin \theta_2 \sin \alpha_2}{y_2 \cos (\theta_2 + \alpha_2)} + \frac{\sin \theta_3 \sin \alpha_3}{y_3 \cos (\theta_3 + \alpha_3)} \right] \quad (24a)$$

The characteristic equations for the chord 1-3 now become

$$y_3 - y_1 = A' (x_3 - x_1) \quad (25a)$$

for the physical plane, and

$$\theta_3 - \theta_1 = -C' (M_3^* - M_1^*) + E'' (x_3 - x_1) \quad (26a)$$

for the hodograph plane. The characteristic equations for the chord 2-3 become

$$y_3 - y_2 = B' (x_3 - x_2) \quad (27a)$$

for the physical plane, and

$$\theta_3 - \theta_2 = D' (M_3^* - M_2^*) - F' (x_3 - x_2) \quad (28a)$$

for the hodograph plane.

The values of the properties for point 3" are found in the same manner as used in the first approximation. This process is repeated as many times as necessary to give a degree of accuracy consistent with the errors in the grid. Each successive iteration makes use of the results of the preceeding one. The point designated as

3" in figure 2 represents the results of the first iteration in the process of determining the point. Although the improvement in accuracy attained after each iteration becomes small, the properties determined at a new point become the initial properties for determining the next point. Therefore, the error accumulates and could possibly be quite large after a number of points have been determined. The iteration process is continued until the change between successive values of  $\theta_3$  becomes less than a designated limit  $\epsilon$ . Therefore, when the term  $|\theta_3' - \theta_3| - \epsilon$  becomes negative, the iteration process for that particular point is finished and all the properties of that point have been found to the accuracy desired.

#### Corner Expansion Calculation

The flow around the sharp corner at the exit of the nozzle may be described by a Prandtl-Meyer expansion (9, p. 600). The size of the grid directly depends on the change in  $\theta$  each time a new characteristic line is generated. In the development of the characteristic grid, the amount of expansion was handled in two different ways. The most desirable method is one which would have a constant change in the value of  $\theta$  for each succeeding characteristic line. Therefore, the change in the angle  $\theta$  between succeeding points found at the lip of the nozzle should be as close to being constant as possible.

In Prandtl-Meyer flow, the following relation is true (10, p. 466).

$$\theta = -\sqrt{\frac{k+1}{k-1}} \tan^{-1} \sqrt{\frac{k-1}{k+1} (M^2-1)} + \tan^{-1} \sqrt{M^2-1} + C_3 \quad (29)$$

The constant  $C_3$  may be evaluated from the initial conditions at the lip of the nozzle. The first method used was to assume a specific change in the Mach number for each succeeding expansion line. Using the new Mach number, equation 29 can be solved for a new  $\theta$ . This is the value of  $\theta$  at the beginning of the new characteristic line. However, the relation between  $\theta$  and the Mach number was not linear; therefore, the change in  $\theta$  each time was not constant as desired.

Another method, that was used with more success, designated a specific increase in the pressure ratio,  $P_e/P_x$ , given for isentropic flow by

$$\frac{P_e}{P_x} = \frac{(1 + \frac{k-1}{2} M_x^2)^{\frac{k}{k-1}}}{(1 + \frac{k-1}{2} M_e^2)^{\frac{k}{k-1}}} \quad (30)$$

If equation 30 is solved for  $M_x$ , the result is

$$M_x = \left\{ \frac{2}{k-1} \left[ \left( \frac{P_e}{P_x} \right)^{\frac{k-1}{k}} \left\{ 1 + \frac{k-1}{2} M_e^2 \right\} - 1 \right] \right\}^{\frac{1}{2}} \quad (31)$$

The new value of  $P_e/P_x$ , after the specified increase has been made, is then substituted into equation 31 and the equation is solved for  $M_x$ . This new value for  $M_x$  is then used in equation 29 to determine the new value of  $\theta$ . With the Mach number and  $\theta$  known and the physical coordinates



given for the lip, all the properties for the new point are known. This method gives good results for values of  $\theta$  up to approximately 25 degrees. For larger values of  $\theta$ , the amount of expansion for each new characteristic line becomes increasingly smaller.

#### Points Next to the Axis of Symmetry Calculations

The points in the characteristic grid that lie next to the axis of symmetry require special consideration since in the solution of the characteristic equations for this point, one of the terms in the hodograph plane for the left running characteristic family becomes indeterminate.

Consider figure 3, which denotes the notation and physical concept of a point that is next to the axis of symmetry. All the properties are known for points 1 and 2. Point 3 represents the unknown point and is located at the intersection of the right running characteristic line from point 2 and the left running characteristic line from point 1. The characteristic equations for the chord 1-3 is the same as for an interior point. The characteristic equations for the chord 2-3, however, involves an indeterminate term. The hodograph equation for the first approximation in finite difference form for the characteristic chord 2-3 is as follows:

$$\theta_3 - \theta_2 = \frac{\cot \alpha_2}{M_2^*} (M_3^* - M_2^*) - \frac{\sin \theta_2 \sin \alpha_2}{y_2 \sin (\theta_2 + \alpha_2)} (y_3 - y_2) \quad (28b)$$

# POINT NEXT TO AXIS OF SYMMETRY CALCULATION

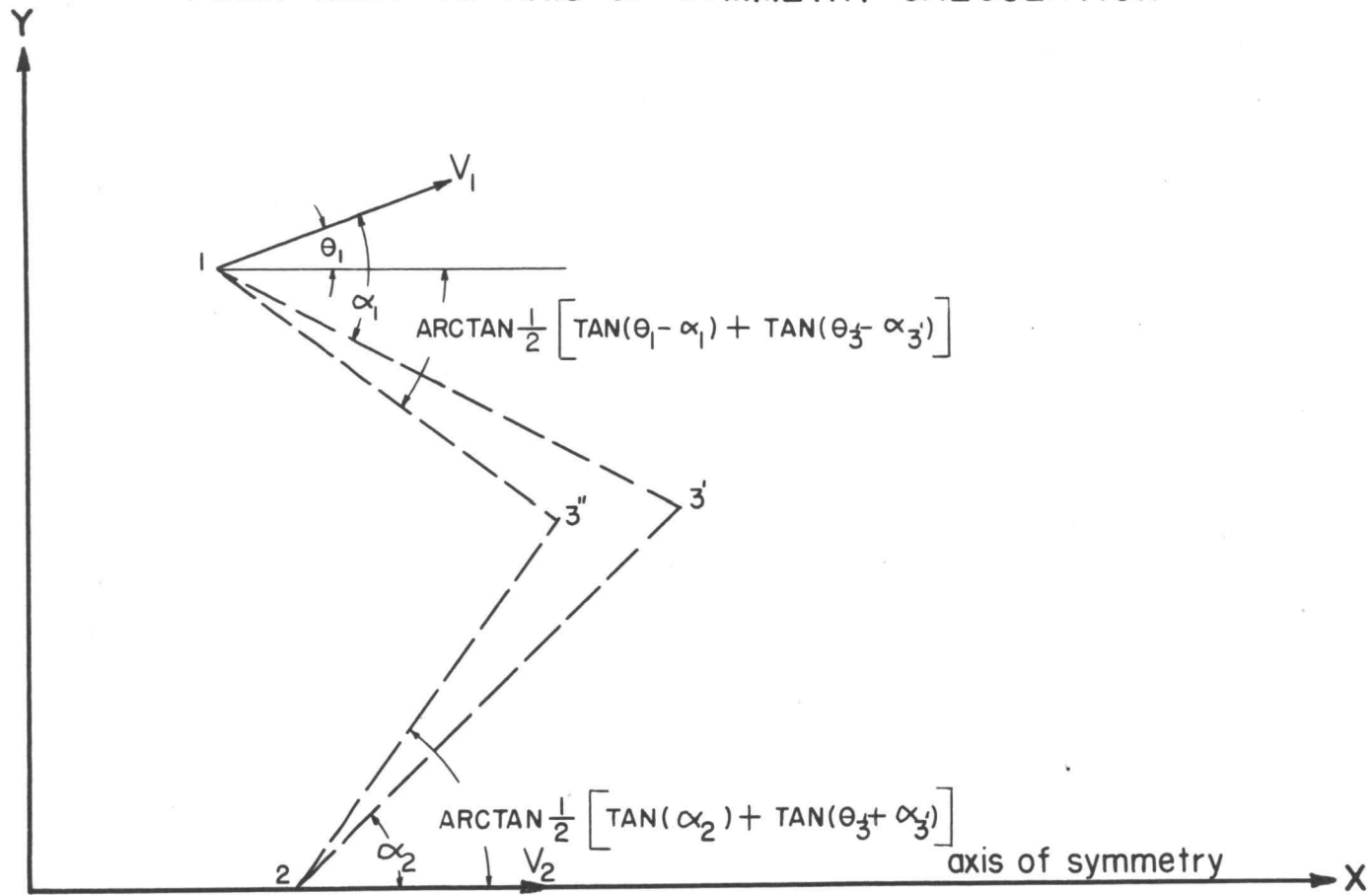


FIGURE 3

Since point 2 lies on the axis of symmetry, both  $y_2$  and  $\theta_2$  are equal to zero. Therefore, the value of  $\frac{\sin \theta_2}{y_2}$  in the last term of equation becomes 0/0, which is an indeterminate form.

The limit of the indeterminate term does approach an approximate value as  $y_2$  approaches zero. The limit of this term results in the following (10, p. 680)

$$\lim_{y \rightarrow 0} \frac{\sin \theta_2 \sin \alpha_2}{y_2 \sin (\theta_2 + \alpha_2)} \sim \frac{\theta_3}{y_3} \quad (32)$$

The value of  $\frac{\theta_3}{y_3}$  being the limit of the indeterminate term assumes that point 3 is close to the axis of symmetry. The closer that point 3 is to the axis of symmetry, the more accurate the limiting value becomes.

1. First Approximation. By inserting the limiting form of the indeterminate term into equation 28b and noting that  $\theta_2$  and  $y_2$  are equal to zero, the hodograph equation for the first approximation of the characteristic chord 2-3 becomes

$$\theta_3 = \frac{\cot \alpha_2}{M_2^*} (M_3^* - M_2^*) - \frac{\theta_3}{y_3} (y_3) \quad (33)$$

If equation 33 is solved for  $\theta_3$ , the result is

$$\theta_3 = \frac{\cot \alpha_2}{2M_2^*} (M_3^* - M_2^*) \quad (33a)$$

The corresponding characteristic equation for the physical plane becomes

$$y_3 = (x_3 - x_2) \tan \alpha_2 \quad (27b)$$

The hodograph equation and the physical equation for the characteristic chord 1-3 are the same as those used in the calculation of an interior point. The hodograph equation is

$$\theta_3 - \theta_1 = -C (M_3^* - M_1^*) + E' (x_3 - x_1) \quad (26)$$

and the corresponding physical characteristic equation is

$$y_3 - y_1 = A(x_3 - x_1) \quad (25)$$

Equations 27b and 25 are solved simultaneously for  $x_3$  and  $y_3$ . These values are then used in equations 33a and 26 which are solved simultaneously to find  $M_3^*$  and  $\theta_3$ . Once these values are found, the first approximation has been completed.

2. Successive Iterations. The following notation is used to simplify the characteristic equations for successive iterations

$$G = \frac{1}{2} \left[ \tan \alpha_2 + \tan (\theta_3 + \alpha_3) \right] \quad (34)$$

$$H = \frac{1}{2} \left[ \theta_3 + \frac{\sin \theta_3 \sin \alpha_3}{\sin (\theta_3 + \alpha_3)} \right] \quad (35)$$

The characteristic equations using the average coefficients along the chord 1-3 become

$$\theta_3 - \theta_1 = -C' (M_3^* - M_1^*) + E'' (x_3 - x_1) \quad (26a)$$

for the hodograph plane, and

$$y_3 - y_1 = A' (x_3 - x_1) \quad (25a)$$

for the physical plane. The corresponding characteristic equations for the chord 2-3 become

$$\theta_3 = D' (M_3^* - M_2^*) - H \quad (36)$$

for the hodograph plane, and

$$y_3 = G (x_3 - x_2) \quad (37)$$

for the physical plane. The properties of point 3' are determined in the same manner as they were determined in the first approximation. This process is repeated until the change between successive values of  $\theta_3$  become less than some specified  $\epsilon$ . Therefore, when the value of  $|\theta_3' - \theta_3| - \epsilon$  becomes negative, the degree of accuracy that was desired has been reached, and the iterations procedure for that point is completed.

#### Point On the Axis of Symmetry Calculation

The points that lie on the axis of symmetry are similar to those that lie next to the axis of symmetry since they both involve an indeterminate term in the characteristic equations for the hodograph plane. Consider figure 4, which denotes the notation and physical concept of a point on the axis of symmetry. The properties of point 1 are known. Point 3 represents the unknown point and lies at the intersection between a right running characteristic line from point 1 and the axis of symmetry.

1. First Approximation. For the first approximation the indeterminate term does not appear since the properties of point 3 do not enter into the characteristic equations.



# POINT ON AXIS OF SYMMETRY CALCULATION

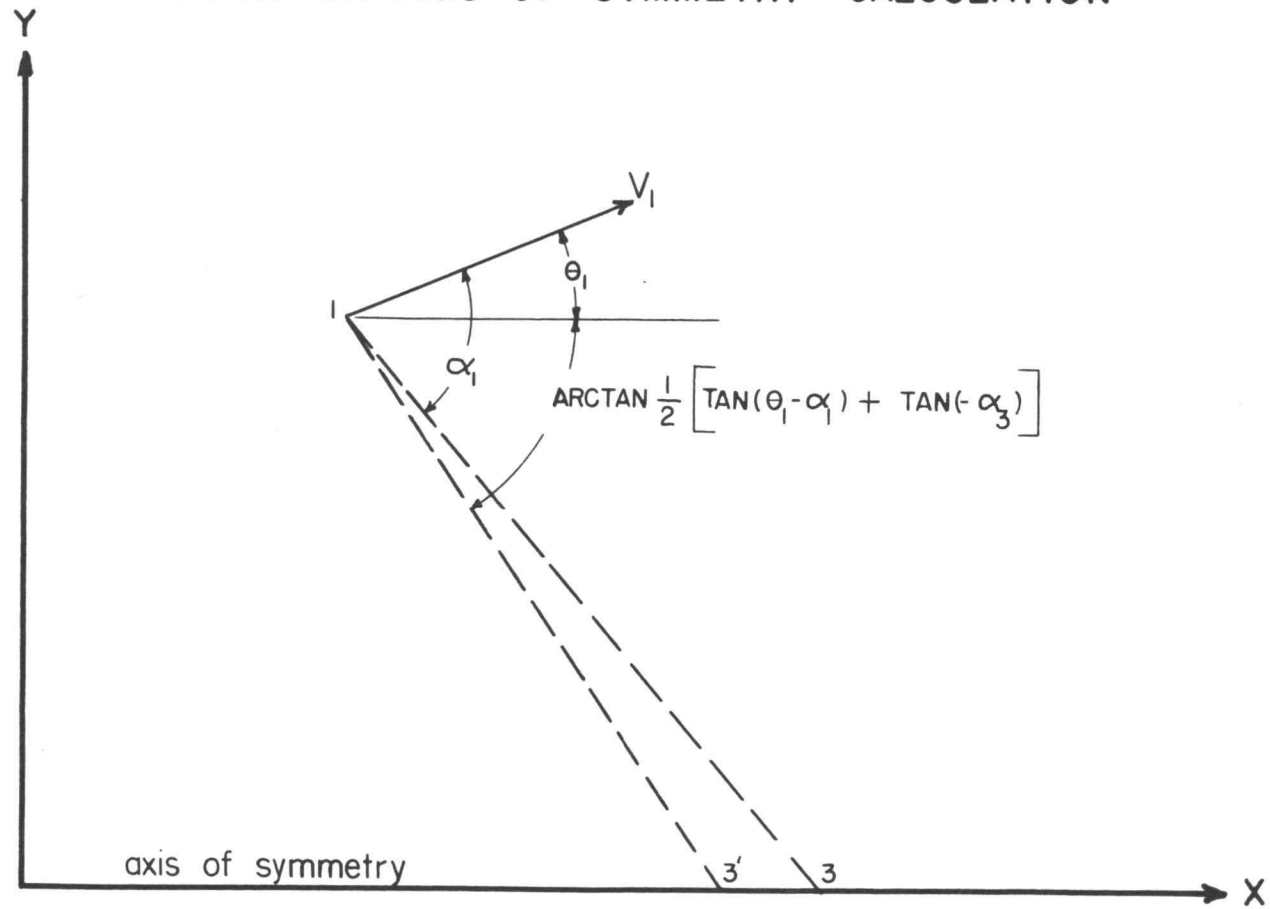


FIGURE 4

The characteristic equations for the chord 1-3 become

$$-y_1 = (x_3 - x_1) \tan (\theta_1 - \alpha_1) \quad (38)$$

for the physical plane, and

$$-\theta_1 = -\frac{\cot \alpha_1}{M_1^*} (M_3^* - M_1^*) + \frac{\sin \theta_1 \sin \alpha_1}{y_1 \sin (\theta_1 - \alpha_1)} (-y_1) \quad (39)$$

for the hodograph plane. The values of  $\theta_3$  and  $y_3$  are equal to zero since point 3 lies on the axis of symmetry. The value for  $x_3$  can be solved from equation 38. Equation 39 can be solved for  $M_3^*$ .

2. Successive Iterations. The average coefficients are used for the characteristic chord 1-3 in the successive iterations. The hodograph equation for the chord 1-3 now becomes

$$-\theta_1 = -\frac{1}{2} \left[ \frac{\cot \alpha_3}{M_3^*} + \frac{\cot \alpha_1}{M_1^*} \right] (M_3^* - M_1^*) + \quad (40)$$

$$\frac{1}{2} \left[ \frac{\sin \theta_1 \sin \alpha_1}{y_1 \sin (\theta_1 - \alpha_1)} + \frac{\sin \theta_3 \sin \alpha_3}{y_3 \sin (\theta_3 - \alpha_3)} \right] (-y_1)$$

The value of  $\theta_3$  and  $y_3$  are both equal to zero from the axis of symmetry condition. Therefore, the last term in equation 40 is indeterminate. The limiting form of the indeterminate term does have an approximate value (10, p. 680). The limit of the indeterminate term results in the following

$$\lim_{y_3 \rightarrow 0} \left[ \frac{\sin \theta_3 \sin \alpha_3}{y_3 \sin (\theta_3 - \alpha_3)} \right] \sim -\frac{\theta_1}{y_1} \quad (41)$$

By replacing the indeterminate term in equation 40 with its limiting value, the result is

$$\begin{aligned}
 -\theta_1 = & \frac{1}{2} \left[ \frac{\cot \alpha_3}{M_3^*} + \frac{\cot \alpha_1}{M_1^*} \right] (M_3^* - M_1^*) + \\
 & \frac{1}{2} \left[ \frac{\sin \theta_1}{y_1} \frac{\sin \alpha_1}{\sin (\theta_1 - \alpha_1)} - \frac{\theta_1}{y_1} \right] (-y_1)
 \end{aligned} \quad (40a)$$

The last term in equation 40a contains the term  $\sin (\theta_1 - \alpha_1)$  in the denominator. This represents a possible trouble spot when the values of  $\theta_1$  and  $\alpha_1$  become equal. This was changed by substituting in the value of  $(-y_1)$  from the physical plane, which changes the term  $\sin (\theta_1 - \alpha_1)$  to  $\cos (\theta_1 - \alpha_1)$ .

The following notation is used to simplify the characteristic equations

$$A'' = \frac{1}{2} \left[ \tan (\theta_1 - \alpha_1) + \tan (-\alpha_3) \right] \quad (19b)$$

$$C' = \frac{1}{2} \left[ \frac{\cot \alpha_3}{M_3^*} + \frac{\cot \alpha_1}{M_1^*} \right] \quad (21a)$$

$$I = \frac{1}{2} \left[ \theta_1 + \frac{\sin \theta_1}{y_1} \frac{\sin \alpha_1}{\cos (\theta_1 - \alpha_1)} (x_3 - x_1) \right] \quad (42)$$

The characteristic equations for the chord 1-3 now become

$$-y_1 = A'' (x_3 - x_1) \quad (43)$$

for the physical plane, and

$$-\theta_1 = -C' (M_3^* - M_1^*) + I \quad (44)$$

for the hodograph plane. The values of  $x_3$  and  $M_3^*$  are found in the same manner as used in the first

approximation. A rapidly convergent iteration process is used with each successive iteration making use of the results of the preceeding one. The convergence process compares the change between consecutive values of  $M_3^*$  with a designated limit,  $\epsilon$ . When the change in  $M_3^*$  becomes less than  $\epsilon$ , the iteration procedure is completed and the desired accuracy has been achieved.

#### Leading Mach Line for a Constant Area Nozzle Calculation

The calculations used in determining the characteristic grid for diverging conical nozzles has been determined. The source flow solution cannot be used for points on the leading characteristic line when  $\Theta_N$  equals zero since the value of  $N$  becomes infinite at this point. Therefore, a separate method was developed for the constant area nozzle. The leading characteristic line for the case of constant area nozzle is represented by a straight line emanating from the lip of the nozzle and having an included angle of  $\alpha$  with the  $x$  axis. Therefore, this characteristic line is a function of the exit Mach number only. The notation and physical concept for this type of nozzle is shown in figure 5. The exit conditions at the lip of the nozzle specify the fluid properties along the entire leading characteristic line. From an examination of figure 5, the physical coordinates,  $x$  and  $y$ , are

## CONSTANT AREA NOZZLE

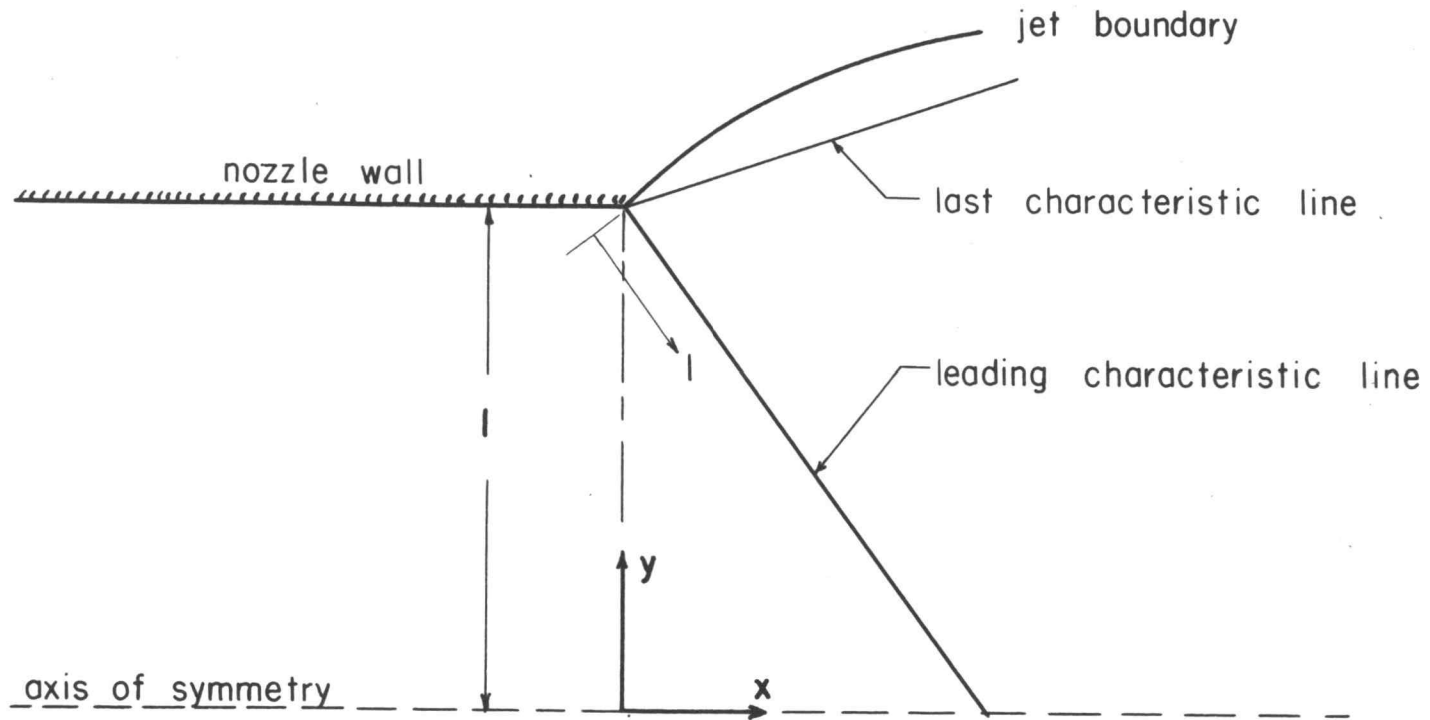


FIGURE 5



$$x = l \cos \alpha \quad (45)$$

and

$$y = l \sin \alpha \quad (46)$$

## CONSTRUCTION OF THE CHARACTERISTIC GRID

All the individual type calculations in connection with the development of the characteristic grid have been considered. The problem now is to combine the different calculations to produce the characteristic grid.

Figure 6 shows the notation and physical concept of the developed characteristic grid. The last characteristic line represents the last right running characteristic line that was calculated before the boundary calculations were used to determine the jet boundary between the nozzle flow and the exterior flow. The section of the characteristic grid between the leading characteristic line and the last characteristic line is called the kernel.

The first step in the development of the characteristic grid is to calculate points along the leading characteristic line. By using the leading characteristic line calculation already considered, the properties of the points on the leading characteristic line can be determined. The number of these points directly affects the size of the characteristic grid produced. The closer the points are together, the finer the characteristic grid will become. The leading characteristic line

# CHARACTERISTIC GRID

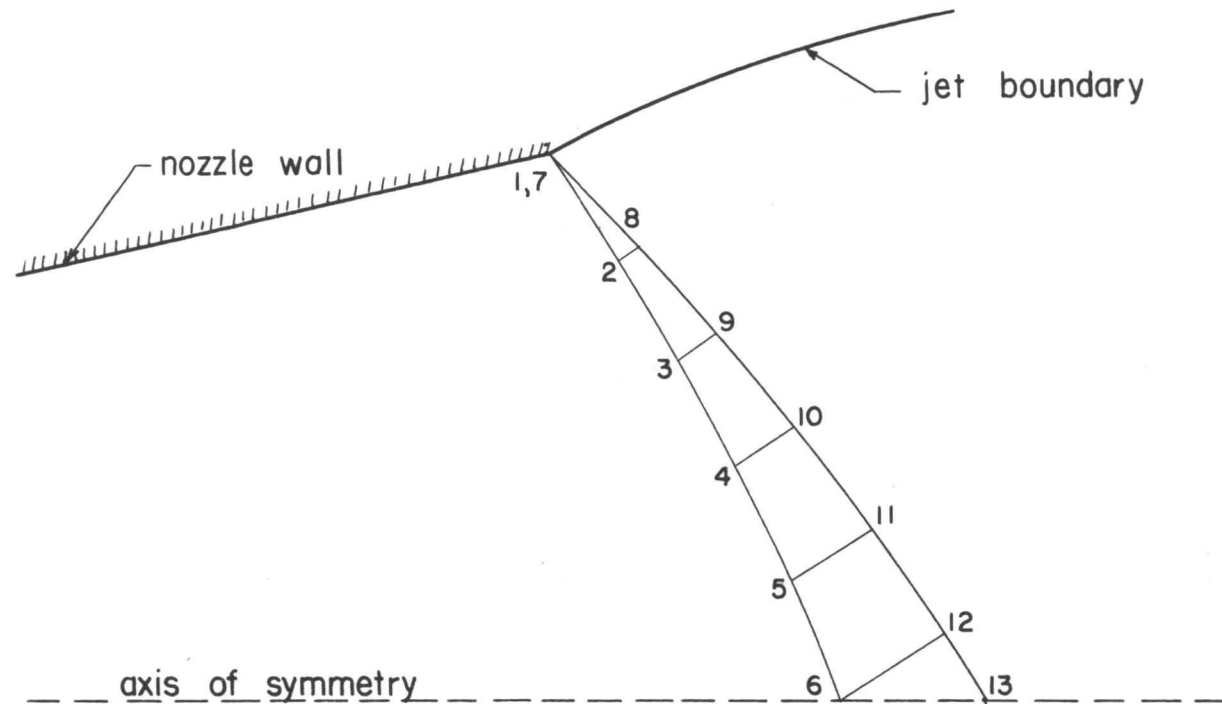


FIGURE 6

is represented by the points 1, 2, 3, 4, 5 and 6 in figure 6. These points can be considered the input data for the development of the kernel of the characteristic grid.

The next step is to use the corner expansion calculations to calculate the start of the next right running characteristic line from the lip of the nozzle. The nozzle flow is expanded around the corner of the nozzle using the specified increase in the pressure ratio,  $\frac{P_e}{P_x}$ . The new calculated point at the lip of the nozzle has the same physical coordinates, but the fluid properties have changed. The new point is represented by point 7 in figure 6.

The next point, which is point 8, represents the intersection of a right running characteristic line from point 7 with a left running characteristic line from point 2. This was the type of calculation that was discussed as an interior point. Therefore, using the interior point calculations, the properties of point 8 can be calculated. The interior point calculations can be used to calculate the properties of points 9, 10 and 11 since they, too, are a solution of the same characteristic equations as point 8.

The properties of point 12 are calculated by using the point next to the axis of symmetry calculations.

The properties of point 13 are found by using the point on the axis of symmetry calculations.

With the determination of point 13, the right running characteristic line represented by the points 7, 8, 9, 10, 11, 12 and 13 has been determined.

The flow at the lip of the nozzle is expanded once more through a specified increase in the pressure ratio,  $P_e/P_x$ , to establish the beginning of the next right running characteristic line. These right running characteristic lines are generated until the last calculated characteristic line is close enough to the jet boundary to use the boundary calculations. The initial properties of the jet boundary at the lip of the nozzle are specified from the free stream and exit conditions. For most cases, the value of  $\theta$  at the lip of the nozzle for the last characteristic line is within 4 or 5 degrees of the value for  $\theta$  from the initial properties of the jet boundary.

The change in  $\theta$  for each new characteristic line is directly related to the size of the grid developed. The grid size is controlled by the change in  $\theta$  for each new characteristic line at the lip of the nozzle and by the number of points on the leading characteristic line. Therefore, it is possible to develop the grid size desired.

The end results of the development of the characteristic grid is the jet boundary. Once the jet boundary is determined, the entire characteristic grid has been developed.



## COMPUTER CALCULATIONS

Since the iteration processes in the development of the characteristic grid are relatively lengthy and numerous, the problem of actually calculating the characteristic grid was programmed on the ALWAC III-E electronic digital computer. The machine time required to accomplish the desired results is of major concern since the program for the development of the characteristic grid for one problem may require several hours for the solution. The method of programming is strictly determined by the ingenuity and ability of the programmer. Although the final program is not optimized, an effort was made to minimize the computer time required for each problem.

### Initial Programs

The interior point calculations that have been discussed in the preceeding section and the boundary point calculations were programmed by Newton (7, p.19). These calculations developed the characteristic grid between the last calculated right running characteristic line and the jet boundary. The interior point calculations are the same for the interior points in the kernel as they are for interior points lying between the last characteristic line and the jet boundary.

The Prandtl-Meyer expansion calculations, which were also programed by Newton, are used in a slightly altered form in the program for the expansion around the sharp corner of the nozzle (7, p. 57).

### Method of Calculation

The sequence of the different calculations, connected together to develop the characteristic grid, was discussed in the preceeding section. The computer programs for the development of the characteristic grid are presented in the appendix.

### Initial Input

The initial input data consists of the following quantities.

1. The specific heat ratios,  $k_e$  and  $k_\infty$ .
2. The initial values of  $\theta_b$  and  $M_b$  at the lip of the nozzle.
3. The nozzle flow parameters  $\theta_e$  and  $M_e$ .
4. The free stream parameters  $\theta_\infty$  and  $M_\infty$ .
5. The designated increase in the pressure ratio at the corner of the nozzle,  $\Delta P$ .
6. The maximum number of interior points to calculate E.
7. The designated decrease in  $\alpha$  to determine the leading Mach line,  $\Delta\alpha$ .
8. The number of points on the axis of symmetry to calculate  $N'$ .

The values of  $k_e$  and  $M_e$  specify the type of nozzle flow while the value of  $\theta_e$  designates the amount of divergence of the nozzle. The quantities  $k_e$  and  $M_e$  designate the type of exterior flow. The values of  $\theta_b$  and  $M_b$  are determined through the use of the Prandtl-Meyer expansion program and denote the initial conditions at the start of the jet boundary. These values also determine the pressure ratio,  $P_e/P_b$ , which must exist to produce such a jet boundary at the lip of the nozzle. The value of  $\Delta P$  is the amount that the pressure ratio,  $P_e/P_x$ , is increased each time a new right running characteristic line is generated at the lip of the nozzle. The quantity  $\Delta\alpha$  designates the amount of decrease in  $\alpha$  for points calculated along the leading characteristic line. The value of  $E$  designated the maximum number of points to be calculated along the leading characteristic line. The quantity  $N'$  represents the number of points to be calculated along the axis of symmetry. The initial input discussed is the input for one entire problem including the calculation of the jet boundary. If the development of the kernel is all that is desired, the properties at the boundary and free stream flow can be ignored.

### Individual Calculations

The combined program was programmed in such a manner that two of the individual calculations can be operated independently. These two calculations are the points on the leading characteristic line program and the corner expansion program.

With the properties of  $\theta_e$ ,  $k_e$ , and  $M_e$  known from the initial input, the conditions at the lip of the nozzle are given. This represents the first point on the leading characteristic line. To calculate the properties of the next point on the leading characteristic line, the value of  $\alpha$  at the lip of the nozzle is decreased by the specified amount  $\Delta\alpha$ . Using this new value of  $\alpha$ , the rest of the properties at the new point can be determined. This process is repeated until the value of  $y$  for a point on the leading characteristic line becomes negative. This indicates that the last calculated point in the physical plane lies below the axis of symmetry. It is desirable to have the last point on the axis of symmetry. The point on the axis of symmetry cannot be found exactly by using this process, but a convergence method was developed which will converge on the point at the axis of symmetry. This convergence method uses the point on the axis of symmetry program to determine

the approximate value of the properties for the point on the axis of symmetry. This is accomplished by using the properties of the last calculated positive point on the leading characteristic line as the input data for the point on the axis of symmetry program. The difference between the value of the calculated  $\alpha$  and  $\alpha$  from the last positive point on the leading characteristic line is determined and divided by one less than the number of points on the leading characteristic line. This new increment of  $\alpha$  is then added to the value of  $\Delta\alpha$ . Using this new value of  $\Delta\alpha$ , the properties of the points on the leading characteristic line are re-calculated. This process is repeated until the difference between  $\alpha$  for the last positive point and the point on the axis of symmetry is less than some designated value  $\epsilon$ . However, if the value of  $\Delta\alpha$ , which will produce a point on the leading characteristic line sufficiently close to the axis of symmetry is known in advance, the convergence process can be eliminated. Since the point on the leading characteristic line program can be used independently of the final program, the value of  $\Delta\alpha$  can be determined before the combined program is used.

The expansion around the sharp corner of the nozzle is handled by the corner expansion program. The pressure ratio,  $P_e/P_x$ , is increased by the quantity  $\Delta p$  and the



properties for the new point at the lip of the nozzle are determined. As was discussed in the preceeding section, the amount of change in the value of  $\theta$  should be constant for each new right running characteristic line. As the value of  $\theta$  get larger, the amount of expansion becomes less. To correct this, it is possible to increase or decrease the value of  $\Delta P$  before the next right running characteristic line is calculated. Therefore, if the amount of expansion begins to become less in value, the value of  $\Delta P$  can be raised to counteract this. One problem in using a value such as  $\Delta P$  to designate the amount of expansion is that there is no way of knowing in advance what the value of the change in  $\theta$  is going to be. The corner expansion program has been programed so that it can be operated independently of the final program. Therefore, it is possible by using this program independently to determine by trial and error a suitable value for  $\Delta P$  that will give the desired change in the value of  $\theta$ .

#### Program Conveniences

While the arithmetic operations of the computer are quite rapid, the type out is much slower. The program stores all the properties of points on any particular right running characteristic line until the whole line has been calculated. It then proceeds to type out the properties for each point on the line, which are  $x$ ,  $y$ ,  $M^*$ ,  $M$ ,  $\theta$  and  $\alpha$ .



Since for a large number of points this is quite lengthy and because the last characteristic line is the desired result, the type out of the characteristic lines in the kernel can be omitted.

In the initial input, the value of E must be known. This value is the maximum number of points that may be calculated on the leading characteristic line. Therefore, it is possible to include only part of the leading characteristic line and develop the characteristic grid from this. If all of the points on the leading characteristic line are to be calculated, the value of E is a number larger than the actual number of points on the line.

The value of N' designates the number of points on the axis of symmetry that are to be calculated. If a certain number of such points are desired, the value of N' represents the number of right running characteristic lines that will include points on the axis of symmetry. After this number of lines has been calculated, the characteristic line breaks away from the axis of symmetry.

The program to develop the characteristic grid of the kernel is independent of the boundary program. When the last right running characteristic line has been calculated, the properties of points on this line are punched on tape. To use the boundary calculations program, the same program that is used to put the properties on tape

is used to store the properties in the correct place. The boundary program is then started as it would be ordinarily.

### Convergence Criteria

The selection of a convergence limit depends on each particular calculation and problem. The size of the grid is a determining factor. The error that the grid size introduces is a function of the distance between successive points. The total overall error involved in any particular problem is equal to error caused by the size of the characteristic grid plus the error in the accuracy of the calculated points. Therefore, even if there is no error in the calculated points, the overall error would still exist. The degree of accuracy of the grid is difficult to establish. It is known that the error introduced by the grid is inversely proportional to the grid size (7, p. 36). Therefore, the larger the characteristic grid size, the more error it introduces. The value of the convergence limit  $\epsilon$  should be made as large as the accuracy requirements will allow since it would reduce the machine time needed to calculate each point.

The type of convergence process used in the calculations was to compare the absolute difference between successive values of  $\theta$  for the point under consideration with a designated limit  $\epsilon$ . Since there are no set rules by which

the value of  $\epsilon$  can be selected for each particular grid size, the value of  $\epsilon$  is steadily decreased until decreasing it any further does not affect the results. The value of the error introduced by the size of the grid varies with various positions in the grid. It can be noticed from figure 6 that the grid spacing is much finer in the vicinity of the lip of the nozzle than near the axis of symmetry. Therefore, the error due to the grid size becomes greater as the points approach the axis of symmetry. To attain a constant over all error, the value of  $\epsilon$  would have to be smaller for points near the axis of symmetry than those near the lip of the nozzle. The value of  $\epsilon$ , however, is fixed and is the same for all the interior point calculations.

Another method of convergence was under consideration. This method made use of a percentage basis to calculate the accuracy of a point. The difference between successive values of  $\theta$  for a point is determined and divided by a function of the grid spacing. This value is then compared with a convergence limit  $\epsilon$  to check for accuracy. This convergence method is denoted by  $|\frac{\Delta\theta}{\theta}| - \epsilon < 0$ . For this particular type flow, the function of the grid spacing can be replaced by  $|\theta|$ . The value for the function of the grid spacing can have other values besides  $|\theta|$ . This was used as an illustration. This method has the ability



to adjust with the size of the grid. If this convergence criteria is put in the same form as the convergence method used in the actual calculations, the result is  $|\Delta\theta| < \epsilon|\theta|$ . If the point is close to the lip of the nozzle, the value of  $\epsilon|\theta|$  is relatively large. As a point approaches the axis of symmetry, the value of  $\theta$  becomes less. The product  $\epsilon|\theta|$  will also become less since  $\epsilon$  is fixed. Therefore, the convergence limit becomes smaller as the grid size increases. By using this method, it seems possible that some machine time could be saved since the convergence limit  $\epsilon|\theta|$  would become larger where the grid was fine, and it would approach the value of  $\epsilon$  used in the first method of convergence for the points near the axis of symmetry. As a result, the points near the lip of the nozzle would not be as accurate as points near the axis of symmetry, but the overall error would be approximately the same.

## CONCLUSIONS AND RECOMMENDATIONS

The development of the characteristic grid for diverging conical nozzles has been completed. The accuracy of the process has been checked against a constant pressure jet boundary and verified (6, p. 15). The problem has been programed on the ALWAC-IIIE electronic computer. It is now possible to develop the characteristic grid and jet boundary completely independent of any precalculated data. With the development of the axis of symmetry calculations, it is now possible to study other supersonic flow problems involving similar axis of symmetry calculations.

The limitations on the method used here to develop the characteristic grid are briefly the following:

1. The flow is axially symmetric, steady, irrotational, and supersonic.
2. The diverging nozzle produces a conical exit flow.
3. The fluid is a perfect gas and has a constant specific heat ratio at constant pressure.
4. The points next to the axis of symmetry in the characteristic grid are close enough to the axis of symmetry for the approximation in their calculation to be valid.

One individual calculation which is needed to solve some types of supersonic flow still remains. This is the solution at a solid boundary which does not lie along the axis of symmetry. Once this is completed, a worth-while study would be the design of supersonic nozzles. The interior point calculations and both of the axis of symmetry calculations could be adapted quite easily to this type of a problem.

The method of convergence using the percentage basis as discussed in the preceeding section seems quite worth-while. The possibility of saving some machine time while attaining the desired results is quite evident.

One direct problem is to study the effect of the various parameters on the jet boundary.

A study of the error introduced by the size of the grid can now be made since it is possible to vary the grid to the size desired.

Through the use of the calculations in this paper and in Newton's, the basic tools for the development of a number of supersonic problems are ready to be used.



## BIBLIOGRAPHY

1. Beek, Allen. Elementary coding manual ALWAC III-E. Hawthorne, Calif., ALWAC Corporation, n.d. 94.
2. Cresci, Robert J. Tabulation of coordinates for hypersonic axisymmetric nozzles. Wright-Patterson AFB, U.S. Dpt. of Commerce, OTS, Polytechnic Institute, 1958. 61 p.
3. Isenberg, J. S. and C. C. Linn. The method of characteristics in compressible flow, I. Steady supersonic flow. Wright Field, U.S. Air Material Command, U.S. Dpt. of Commerce, OTS, 1947. 217 p. (Air Material Command Technical Report No. F-TR-1173A-ND) (Microfilm)
4. Johannesen, N. H. Ejector theory and experiments. Kobenhavn, Danish Academy of Technical Sciences, 1951. 176 p.
5. Love, Eugene S. and Carl E. Grisby. Some studies of axisymmetric free jets exhausting from supersonic nozzles into still air and into supersonic streams. Washington, National Advisory Committee for Aeronautics, 1955. 178 p. (NACA Research Memorandum RM L34L31)
6. Love, Eugene S. and Louise Lee. Shape of initial portion of boundary of supersonic axisymmetric free jets at large pressure ratios. Washington, National Advisory Committee for Aeronautics, 1958. 29 p. (NACA Technical Note TN 4195)
7. Newton, John. An application of the Newtonian boundary condition to supersonic jets exhausting into a hypersonic stream. Master's thesis. Corvallis, Oregon State College, 1959. 61 numb. leaves.
8. Sauer, Robert. Introduction to theoretical gas dynamics. Tr. by Freeman K. Hill and Ralph A. Alpher. Ann Arbor, J. W. Edwards, 1947. 222 p.
9. Sears, William Rees. (ed.) General theory of high speed aerodynamics. New Jersey, University of Princeton, 1954. 758 p.

10. Shapiro, Ascher H. The dynamics and thermodynamics of compressible fluid flow. New York, Ronald, 1953. 2 vols.
11. Wang, C. T. and J. B. Peterson. Spreading of supersonic jets from axially symmetric nozzles. Jet Propulsion 28:321-328. 1958.

## APPENDIX

Subroutines

All the calculations are programed on the ALWAC-III E electronic digital computer. The programs use the floating point subroutines. The subroutines used are as follows:

- |                |                   |
|----------------|-------------------|
| 1. sin         | 7. add multiply   |
| 2. cosin       | 8. addition       |
| 3. square root | 9. multiplication |
| 4. arctangent  | 10. division      |
| 5. exponential | 11. input         |
| 6. natural log | 12. output        |

Programs

The combined program has two programs which can be used independently. These two programs, the point on the leading characteristic line and corner expansion, will be considered separately, but must be included with the rest of the combined program to solve a complete problem. The Newtonian boundary program and the Prandtl-Meyer program is listed in Newton's thesis and will not be included (7).

Point on the Leading Characteristic Line Program

The program is started with 6500.



1. Input data. The input data consists of  $k_a$ ,  $\theta_a$ , and  $M_c$ .
2. Output data. The output consists of  $x$ ,  $y$ ,  $M^*$ ,  $M$ ,  $\theta$ , and  $\alpha$  for every point on the leading characteristic line.
3. Location of convergence limit. The limit,  $\epsilon$ , is located in channel 7d, word 1f.
4. Modification. When this program is used with the combined program, an unnecessary carriage return needs to be deleted. To delete the carriage return, insert the following word

72    0e    00000000

## COMPUTER PROGRAM

65  
 83668567 f706795f 872a3025 00005b53  
 795bf701 83761126 5b53791b 7917a508  
 555f7844 8366a508 a5081160 1160495c  
 f706872e 11603a02 87133000 5b437953  
 795b1160 79532f30 79191160 2f301120  
 48441788 791b1160 c5498712 8b9e7e02  
 550c7906 87293016 41417917 0e197e61  
 f701784a 790d1160 116c872a 8db66f6f  
 65 34b54504

66  
 793f1160 79021160 414c7951 5b564144  
 49445b43 49478712 a5081160 79521160  
 4153793f 4149793b 494d8712 30005b4b  
 a5081160 a5081160 4149795a 7952a508  
 49453a9c c54c872a 11600011 1160494b  
 4144793b 5b4c414c 5b4c872a 81681100  
 11604946 79511160 795aa508 31b8027e  
 87294146 494b5b53 11604940 30246161  
 66 32b59fa7

67  
 53150f80 6689d994 53d45468 53050f80  
 53bd0000 53c50000 53176000 45400000  
 6689d994 53151a00 00000000 00000000  
 00000000 00000000 00000000 00000000  
 00000000 2a3d7e6f b32b6f7e 86000000  
 25b87e61 0a097e6f 8a000000 6e3be8d3  
 b0286f6f 8e000000 beb27e01 5b6da014  
 00000000 14087e61 07126f6f 58040000  
 67 b0beef7c

68  
 30005b53 5b4e0000 41447955 a5081160  
 795d1160 79551160 a5081160 494b3000  
 494b5b46 871b30bc 30005b4e 5b5c791f  
 4159795d 79321160 795e1160 11604950  
 a5081160 494b8718 871b3099 41505b4b  
 494e8718 414d7912 791a1160 791fa508  
 414b7930 1160872a 872a301a 83691120  
 1160872a c54e5b53 5b4b795e a08f6f7e  
 68 570b77eb

Figure 7

69  
 1160494c 313a4157 41577933 872b792c  
 41475b40 79371160 a5081160 4d7a5b56  
 793b1160 5b473000 494f414f 81701100  
 30045b53 7937a508 5b4a792f beb27e61  
 793ba508 11603000 1160494a 2a3d7e61  
 11608713 793f2f3a 5b414157 b1296f7e  
 30007909 79331160 792fa508 b42c7e6f  
 1160872a 494a5b49 11603000 9ed00000  
 69 5947a625

70  
 794a1160 5b57791b 00000000 4141790f  
 495b872a 1160494a 8371414f a5081160  
 794a2f3a 87123000 11138712 83711120  
 415b791f 791ba508 414a7917 0b1e016f  
 11603a00 1160872a a5081160 81721116  
 4156791f 5b4c7917 872a5b4c 1699016f  
 a5081160 1160494b 790f1160 9185026f  
 494e3000 1d02118a 494a8712 1c907e61  
 70 45a19ed8

71  
 872a5b5c 414d793b 5b487933 818c1199  
 793f1160 a5081160 11603000 8172118c  
 2f305b4a 49483023 5b537933 00000000  
 793fa508 5b4c7937 a5081160 583a007e  
 1160494a 1160494c 30065b4c 32a6616f  
 5b454156 5b444156 792f1160 bdb17e6f  
 793b1160 7937a508 87293018 293c6f7e  
 494c5b4d 11603000 79291160 b028616f  
 71 95adae5d

72  
 49278b71 79422f30 83697917 81771100  
 0006110d 5b4f791f 49367908 5b9a0061  
 494a11aa 1160494f 493d8b69 494b3000  
 00005504 414f5b57 00000000 1188f701  
 872f793a 791fa508 836611a5 494c8172  
 40501160 11604949 79075b42 81701184  
 792ff701 8368791b 1160494f 494b1113  
 1710872a 49278b68 79031100 95896f61  
 72 e6addec4d

Figure 7 Continued



76  
49434154 1b00555b 494911b7 79374940  
5b497959 872f7939 f701179e 2800492b  
a5081160 40491160 7906f701 8b8c8374  
2f305b57 795bf601 872a4141 11af8165  
7955a508 17057905 5b57791f 113a5b40  
11604944 f701872a 11604941 8165791f  
00001181 41495b58 838c11b4 11090000  
7951f706 795c1160 414011b3 58000000  
76 4d6a141d

Figure 7 Continued

Corner Expansion Program

The program is started by 6c20

1. Input data. Input data consists of the following:  
 $k_e$ ,  $k_w$ ,  $\theta_b$ ,  $M_b$ ,  $M_e$ ,  $M_w$ , and  $\Delta P$ .
2. Output data. The output is as follows:  $M$ ,  $M^*$ ,  
 $\alpha$ ,  $w$ , and  $\theta$ , where  $w$  is a function of  $\theta$ .
3. Modification. The carriage returns are deleted  
by inserting the following words:

6b	0c	00000000
6o	18	00000000
6o	1c	00007921

## COMPUTER PROGRAM

6a  
 30005b1b 87124102 a5085b05 490e5b0e  
 a5081160 790b1160 1160410e 411b790a  
 871b4131 333a872a 30065b0b a5081160  
 30001160 790ba508 1160410e 490f793b  
 4903872a 1160490b 30025b1f f7025552  
 79164922 41015b05 a5081160 780af706  
 492a7912 79071160 410a3098 7906f701  
 4950113d 41073034 5b031160 1757110e  
 6a 7alf17a5

6b  
 014c1400 014c1424 6689a994 014c5416  
 014c541c 014c5424 58000011 c65d6f6f  
 014ce000 4b41d8ca 4f437e6f d1496f02  
 793bf701 1714791d 5ace616f 3aae616f  
 5552872f 4922492a 491b1141 4903872a  
 795a4010 79134950 30005b04 82000000  
 11607906 836a1120 482f6f7e 00000000  
 f701110d 5b033055 31a1616f 86000000  
 6b d9f1306b

6d  
 816b856a 11604902 30005b03 c51b872a  
 793bf701 791f411e 1160410f 5b00411e  
 55347806 2f30a508 30005b03 791a1160  
 f706872e 5b001160 1160410f 411a1140  
 79321160 491e3a50 5b1f3034 6e3be8d3  
 480617a8 41177937 a5081160 00b9006f  
 872a4102 11604937 8718413b 5b6da023  
 5b33791e 7937413f 30001160 00a6006f  
 6d f34f1e65

60  
 8361571f f705571f 5b3e7917 11604936  
 793ff701 793bf701 a5081160 5b2f4133  
 7824f707 7828f705 493a5b28 791b1160  
 872e791f 1705793f 79372f30 00000000  
 1160482c f7015b28 79131160 83166f61  
 17080000 4137872a 49333000 0a1d6f61  
 00000000 79171160 5b3e7913 002c007e  
 f7017921 492f3031 a5080000 00040090  
 60 0da0accl

Figure 8



61

014c1400 014c5400 0149a400 6689d994  
 53177400 150ca894 4911c814 6689d994  
 00000000 00000000 00000000 00000000  
 8562412f 412f1160 00000000 00000000  
 492f5b33 49321140 0038007e 00000000  
 79321160 6e3be8d3 00000000 86000000  
 49338729 1a0e7e61 00000000 580000dd  
 791d112d 91097e61 82000000 5b6da0c6  
 61 eb9ac444

62

8163872a 795b1160 4157793f 41535b37  
 41295b29 87293055 1160872a 791f1160  
 795f1160 794c1160 c5577932 01146f6f  
 492e304d 4957413e 2f3a4157 00de0061  
 79372f3a 79451160 795ba508 00000000  
 795fa508 49538713 11603008 00000000  
 1160493e 3000793b 5b3e794f d6456f6f  
 30005b33 1160c53e 11604926 d84c616f  
 62 29ce07b8

63

30008713 5b3730c9 49205b20 a5081160  
 79561160 793d1160 79262f30 49274129  
 c525872a 5b533099 79391160 790e872f  
 5b3a412e 793da508 49233a8f 1160793b  
 794b1160 11603040 41357939 f7017911  
 49535b36 87297909 a5081160 41240000  
 412e794b 11604924 492330d4 85641160  
 a5081160 872a7926 5b2b791f 0700617e  
 63 98fc2522

64

793bf701 793bf701 491d8963 872a1182  
 872a5b25 41277901 79571147 491d8963  
 4135795f 1160872a 8361551b 1bcb7943  
 11603041 412a5b29 7844482e 491d8963  
 872f791a 795fa508 170e8d6e 856211c0  
 1160793b 11604929 81601194 872a7926  
 f7014123 00000000 83781139 00040000  
 794c1160 8163795e 872a1182 d5cc617e  
 64 eda37e2a

Figure 8, Continued

6c  
 8160793f 792f4940 79271160 411e1144  
 4910856e 8d6d856a 49577953 be26617e  
 793b491c 792b4953 f706872e 836c1131  
 1100816d 836d1138 794d1160 816b856a  
 79374900 8979856e 494f872a 836c113c  
 896d7933 790f495f 11235b4f 816b4938  
 836d1120 790e495b 7927a508 836c11ac  
 8d6e856d 5b03411b 1160494b 11604844  
 6c f7895649

6e  
 86ecccc 8ac7be13 00000014 8e000000  
 5b567947 872a5b3b 00000000 d4c87e7e  
 1160493f 795e1160 83785b04 86000000  
 5b1e4100 871b3032 793f1160 768f5c28  
 7947a508 791d1160 860b620b 53d4b400  
 1160493b 872a0045 8a000000 96b66dbf  
 8718414b 4952413f 86000000 aall16fa  
 79551160 114a0000 464d6f6f 96b66dbf  
 6e aac07e21

78  
 5b043025 79201160 49468d64 872a7926  
 793fa508 49410000 81637923 79571147  
 11603000 00008164 491d8963 872a1182  
 5b1f793b 7937490d 817f1100 412a5b29  
 11603000 79334906 495d8d63 8b90115a  
 5b52793b 8964110a 856e8179 11595b29  
 a5081160 8564792f 836c11b2 3eb06f61  
 817f1118 494d7927 872a1182 a8206f7e  
 78 9a1887a2

7f  
 836c791f 11604913 11608729 8361551b  
 49368b6e 4140791b 30001121 414b5b4f  
 85647903 2f3a7917 836c4936 82196f7e  
 494a838c a5081160 8b6c8378 8a000000  
 11a41b14 30005b0f 791e494a 250a0337  
 7907110a 790b1160 8d64793e 11816161  
 3128791b 30005b13 85631132 86000000  
 2f3a7917 790ba508 8390551b 11235b4f  
 7f fd7f463f

Figure 8, Continued

8c  
49488185 492f8b8c 5b077903 3e866161  
1187793f 8376113e 1160490b 86000000  
49568a64 792f4943 898e0000 96a00000  
1bac793b 79334941 11272800 86cccccc  
49568a64 2800492b 490b11a1 763be8d3  
11147940 8b8c8176 7923a508 8abae147  
49377941 1103494c 872a1160 85621140  
49337943 872a410b 30001191 81601194  
8c 218b5d9f

Figure 8, Concluded



Combined Program

Type 7elf to start the program.

1. Input data. The input data consists of the following:  $k_e$ ,  $k_o$ ,  $\theta_b$ ,  $M_b$ ,  $M_e$ ,  $M_\infty$ ,  $\Delta P$ ,  $\theta_e$ ,  $\Delta\alpha$ ,  $E$ , and  $N'$ .
2. Output data. The output data is as follows:  $x$ ,  $y$ ,  $M^*$ ,  $M$ ,  $\theta$ , and  $\alpha$  for each point in the characteristic grid.
3. Data Storage. The points on each right running characteristic line are stored in channel (f0-Z) where Z is the number that the point occupies on the characteristic line. One point is stored in each channel. Point number 1 will be located in channel ef, while point number 2 is located in channel ee, and so forth. The points are numbered as shown in figure 6, with point number 1 representing the point at the lip of the nozzle.
4. Location of Convergence Limit. The location of for the point on the leading characteristic line has already been given. The corresponding location for the point on the axis of symmetry program is the same. For the interior point calculations, f, is located in channel 5e, word 37. The location for the point next to the axis of symmetry program is channel 8a, word 2f.

5. Modification. If the type out of a right running characteristic line wants to be omitted, put jump switch 1 in the forward position. If a new value of  $\Delta P$  wants to be introduced into the program, set jump switch 2 in the normal position.

## COMPUTER PROGRAM

```

42
014c1400 014c1424 014c5424 014cf400
00000000 82000000 00000000 00046000
86000000 00000000 00000000 00000000
00000000 00000000 00000000 00000000
00000061 0013007e 00000000 00000000
92916f61 00000000 001e006f 00000000
861d0202 0087006f 00000000 00000000
00000000 00000000 00000000 00000000
42 269c436a

```

```

53
8712414f 415f791b 2f305b4e 4155790f
791f1160 a5081160 79131160 a5081160
c540414f c5417917 49547913 b8ac017e
791fa508 415f1160 a508415e 249e0201
1160c51f c51b872a 5b5f1160 160a6161
5b40872a 5b417917 49558712 1d117e02
791b1160 a5081160 3000790f 091c017e
49408712 4941794f 1160c556 90080201
53 75da2c75

```

```

54
81531100 1160333a 1160872a 5b1f7933
872a333a 4157872a 5b1b7937 a5081160
790b4156 793fa508 11603a00 81553a00
11604946 11604944 41567937 41571100
8712790b 8712793b a5081160 2b3e6f7e
a5084154 414e1160 3a00415b 36aa7e6f
1160c557 c53f793b 79331160 a2390202
793f4154 a508415e 4943413f ada17e02
54 2eecla46

```

```

55
8356791f 79084d7a 79462f30 00001160
1160414b 791f414a 5b447917 302fc559
3a0d791f 5b441160 a5081160 5b467913
a5081160 491f795a 301d5b1f 11600000
4942794b 2f305b46 791ba508 2820616f
2f305b5b 790e4d7a 11604954 0e076161
791b1160 791f1160 795a2f30 961c7e61
491f872b 491f872a 5b547917 10847e7e
55 31fbc7d0

```

Figure 9



56

315b7913 5b41415c 4913795e 79074d7a  
 a5081160 793b1160 2f305b4e 791b4143  
 49554140 49415b40 7937a508 5b591160  
 5b41793f 30be793b 1160491f 872a3000  
 1160491b a5081160 872b792d 83571120  
 5b40414c 4917794a 4d7a791f ae226161  
 793fa508 2f305b54 41425b13 3529617e  
 11604940 79371160 1160491f beb07e61  
 56 795b580f

57

5b1f793f 5b41793b 5b3f7933 93167e61  
 11603a00 a5081160 11604958 0a9d7e61  
 4117793f 30005b5e 11000000 95096f6f  
 a5081160 79371160 879a6161 9c906f7e  
 49568158 493f7943 92867e7e 88a66161  
 795c2f30 2f305b59 1d910102 bd316f61  
 5b56793b 7937a508 89010201 29bc6f61  
 11603000 11603000 180c6161 30a47e61  
 57 f476d9a9

58

41485b48 30005b3b 5b337927 790a1160  
 7933a508 792b1160 a5081160 49575b48  
 11603a9b 49337952 492f3007 412b7923  
 4153792f 2f305b37 79482f3a 872aa508  
 1160493b 792ba508 79231160 11608713  
 41565b56 1160301e 87293000 30007908  
 792fa508 5b487927 79151160 1160c559  
 11604937 11603000 492b412f 81591100  
 58 e74be562

59

872a7959 c5514123 5b3a7932 792ea508  
 2f305b58 793aa508 11604936 11604919  
 793e1160 1160c53e 5b3e4151 835a4148  
 49274158 41277936 7932a508 5b48793f  
 5b59793e 1160c53a 11605b46 1160491e  
 a5081160 41277936 30a1792e 794b1120  
 49238712 a5081160 1160491d 3aaa617e  
 793a1160 c550872a 41365b44 a2b0616f  
 59 30502a86

Figure 9, Continued

59  
 872a7959 c5514123 5b3a7932 792ea508  
 2f305b58 793aa508 11604936 11604919  
 793e1160 1160c53e 5b3e4151 835a4148  
 49274158 41277936 7932a508 5b48793f  
 5b59793e 1160c53a 11605b46 1160491e  
 a5081160 41277936 30a1792e 794b1120  
 49238712 a5081160 1160491d 3aaa617e  
 793a1160 c550872a 41365b44 a2b0616f  
 59 30502a86

5a  
 2f305b5b 11604916 11603000 3000872b  
 793fa508 792c4d7a 5b17791b 792e4d7a  
 11605b1e 795a2f30 11604954 5b1d795b  
 30b1791f 5b1d7916 3aaf795a 11604955  
 1160491a 11604917 2f30791b 815b8712  
 872b7916 791d872a a5081160 835c1100  
 4d7a414a 2f305b19 30005b45 0023006f  
 5b19791a 791fa508 793b1160 a8936161  
 5a b6895495

5b  
 4159793f 11604908 3a004155 00000000  
 1160c500 3a004151 7933a508 5b404149  
 4159793f 79371160 11604950 792b1160  
 a5081160 3a004155 5b004104 30005b45  
 c5044158 7937a508 792f1160 792ba508  
 793b1160 11604951 3a004156 11604149  
 5b04872a 5b084150 792fa508 49495b41  
 793ba508 79331160 11604949 79271160  
 5b 57c21881

5c  
 30105b45 49515b43 4924795e bc346f61  
 7927a508 793e1160 2f305b4e a8206f61  
 11604150 300d5b45 791ba508 970f6f61  
 49505b42 793ea508 1160492c 9e167e7e  
 79231160 1160815d 794a2f30 8a027e7e  
 309c5b45 491f795a 5b547917 950d7e7e  
 7923a508 2f30791b 00991160 81186f02  
 11604151 5b541160 b1296f61 10840201  
 5c 5c650892

Figure 9, Continued



5d  
 491b872b 79294d7a 5b507917 4913872b  
 79204d7a 79345b1b a5081160 790a4d7a  
 792c5b49 41511160 30205b1f 794e4113  
 414c1160 4929793a 79131160 5b491160  
 49207934 4d7a7929 4956835e 0312617e  
 4d7a7920 5b1f4124 2f305b4e 0a006161  
 5b5e4150 1160491f 7913a508 ae226161  
 11604934 872a4149 00ac1160 00000000  
 5d 2bc50d74

5e  
 4917791e 2f3a793b 8150570f 00000000  
 4d7a7917 a5081160 17a68cf0 00000000  
 41515b1b 1d39793f c30f1704 00000000  
 1160493f 49588158 792ff703 5b6da000  
 872a2f30 83571100 835f1120 00060000  
 5b58793b 00000000 00000000 65000000  
 11600000 5733785a 00000000 29b86161  
 2d307937 486017b9 00000000 00000000  
 5e aad6e304

80  
 8582872a 791b1160 7917a508 790f1160  
 41565b58 3a004155 1160c541 c51f415f  
 791f1160 791ba508 41407913 83811120  
 49553000 11604955 1160333a a4070102  
 5b57791f 414e794f 4141872a 9a8e7e02  
 a5081160 2f3a7917 7913a508 86990161  
 49544156 11604940 11604940 8d057e61  
 79582f3a 87124140 8712415f 180c7e61  
 80 eebc8b61

81  
 790fa508 793b1160 7937a508 11604943  
 1160872a 2f305b3f 11603000 3a00415c  
 5b1f793f 793ba508 5b3b7933 81831100  
 11604942 11603000 11604944 84a37e7e  
 41405b4a 794b2f3a 41425b58 baae7e7e  
 793fa508 79371160 7933a508 a6396161  
 1160493f 493b4140 11603a00 ad25616f  
 415a5b42 79422f3a 4157792f b8ac6f7e  
 81 08d39c43

Figure 9, Continued

82  
 7e2d6b88 7ed77ad0 7eb910ba 86f022d7  
 8b49a51c 76838c95 8a0f995e 8b6cdee0  
 8b6967a3 961f2fd2 8abcl49e 7b88def1  
 8a0344be 7e0f399b 73306fa5 7e864a85  
 82f4e834 73cf9a40 870b247f 6e0cff38  
 83555555 7aaaaaa8 86ccccc 8a000000  
 86000000 6e3be8d3 8b49a51c 76838c95  
 8a0f995e 8b6cdee0 8b6967a3 961f2fd2  
 82 6acdda52

83  
 792fa508 791b1160 2f3a7917 3a004141  
 11604950 491f3a00 a5081160 790f1160  
 8712414f 414c791b 49178712 83841120  
 791f1160 a5081160 414e7913 2c0b6f7e  
 c551414f 49523000 1160872a 9e926f02  
 791fa508 5b507917 00005b51 0a996161  
 1160333a 1160491b 7913a508 11057e7e  
 4151872a 4144794a 11604953 98100102  
 83 6b17alb7

84  
 49533000 5b1f793b 7937a508 792f1160  
 5b17790f 11603000 11603000 49484146  
 a5081160 5b43793b 5b427933 81851100  
 3a00414b a5081160 11604945 08276f6f  
 793f1160 3a00411b 4146795c 3eae616f  
 30005b4e 79371160 2f3a7933 a639617e  
 793fa508 49464144 a5081160 31a56161  
 11603000 795a2f3a 30005b50 bc34617e  
 84 f59e83e9

85  
 5b46792f 5b58791b 2f3a7917 790a1160  
 a5081160 11603099 872a1160 c5498712  
 493f3012 5b3b791b 87293007 41497913  
 5b54791f a5081160 79081160 83861160  
 1160493b 491f8729 872a3000 a8200201  
 41555b3f 30007905 5b587917 1e0a7e61  
 791fa508 11604947 a5081160 11857e61  
 11602f30 411f7958 87133000 9e906f6f  
 85 f74aeae5

Figure 9, Continued

86

c5414149 793b1160 a5081160 11608712  
 7913a508 3a004157 c53b4148 4937792f  
 1160872a 793ba508 79331160 81871100  
 5b41793f 1160495e 872a5b3b 04a30261  
 11603a00 5b53414b 7933a508 b62e6f02  
 4146793f 79371160 11604941 2639027e  
 a5081160 493f8712 41485b2f ad257e61  
 49515b52 41497937 79492f3a 3eb07e7e  
 86 dfa754bd

87

a5081160 11603a00 5b407913 1160495b  
 c5334137 4145791b 11603a00 83884149  
 791f1160 a5081160 41577913 5b481120  
 c52f872a 5b3f7917 a5081160 839a617e  
 5b33791f 11603a00 494d5b51 12867e61  
 a5081160 41577917 4157790f 1d917e61  
 491f5b41 a5081160 11605b50 0d817e7e  
 412f791b 495d411f 790fa508 180c7e01  
 87 f8a495ef

88

793f1160 493b5b41 7933a508 872a794d  
 491b8712 413f7937 11604157 2f3a8189  
 793fa508 11605b48 3abe792f 414a1100  
 1160c53f 7937a508 11604941 84ae6f7e  
 411b793b 11603a00 872b792a a6b9617e  
 11605b3f 41577933 4d7a794b b1a9617e  
 793ba508 11604951 41415b5a 21b47e01  
 872a1160 413b5b42 11604937 ac240261  
 88 fad5b8b9

89

792fa508 4944415e a5081160 5b1f790b  
 11605b37 5b4c791b 5b5d7913 838a1160  
 791f1160 a5081160 11605b4e 2c206161  
 4933794d 491f415b 7913a508 031a6161  
 2f3a4141 5b5c7917 11605b51 928a616f  
 791fa508 1160491b 790f1160 0695616f  
 11605b33 794a2f3a 5b1b790f 0d016f7e  
 791b1160 41447917 a5081160 980c6161  
 89 9b39b85c

Figure 9, Continued



8a

4917415b 5b41793b a5081160 838411a7  
 5b5e790b 11604945 49517948 5b514159  
 a5081160 795c2f3a 2f3a7933 818b1100  
 5b17793f 4146793b 11602a30 65000000  
 11604946 a5081160 792f2f3a baae6161  
 795a2f3a 5b5b7937 7933a508 26b9616f  
 4144793f 11607951 11601a27 35a5616f  
 a5081160 2f3a7937 79514948 21b0617e  
 8a 280585bc

8b

791f1160 791fa508 49485b49 f701171a  
 49485b49 872a1160 41597913 7908f701  
 4159791f 2a30791b 11604949 1b007941  
 a5081160 2f3a7917 5500784a 838c1120  
 4949551b 11601a95 4860178e 588a007e  
 784a4860 118b5b41 872f5500 02917e61  
 17148395 41597917 40607910 00060000  
 11b10000 a5081160 11607913 10047e7e  
 8b 85334eal

77

872a414e 411f791b 79131160 1160c51b  
 5b57791f a5081160 4947414c 837a4149  
 1160494f 872a0a00 5b407913 793f1160  
 79492f3a 415e7917 a5081160 8396027e  
 791fa508 1160495a 5b53790f 12066f61  
 1160491f 794b2f3a 11604952 9d917e7e  
 8712791b 7917a508 8712414f 099c0201  
 1160c55e 11605b4a 790fa508 9488616f  
 77 62d6d781

7a

872a5b1b 794a2f3a 11605b4f 5b44792b  
 793fa508 79371160 792f1160 817b1100  
 11603a00 5b5d7937 3a004152 043e6f7e  
 415e793b a5081160 792fa508 b22a7e61  
 11603a00 493f5b53 11604944 a2b9617e  
 414b793b 41407933 5b564145 31296f61  
 a5081160 11605b3f 792b1160 3eb07e7e  
 495d4147 7933a508 493b4144 a8206f02  
 7a 54ecbfe8

Figure 9, Continued

7b

a5081160 5b33791b 7913a510 c51b4151  
 49375b3b a5081160 1160872a 790fa508  
 791f1160 491f8729 5b537917 839d1160  
 49335b37 79131160 a5081160 20030201  
 4146791f 494d872a 87137913 00861a11  
 a5081160 79532f3a a5081160 129d7e61  
 2f3a4153 411f7917 c5518712 09017e61  
 791b1160 11608729 790f1160 180c7e6f  
 7b 220cf8aa

7c

5b514157 118e898c 89718165 817d1109  
 793f1160 1b008168 11250000 5b414157  
 494f7947 79374907 793fa508 8172118c  
 494a791b 89688169 119a3000 58000000  
 494c2800 7933491d 79532f3a 494a5b49  
 494e494b 79274916 110e818c 494b3000  
 00008172 89698171 118e0018 171011a5  
 793b491c 792b4907 00001100 0028007e  
 7c b87accad

7d

5b3f792b 11602d3a 790f4922 001e0061  
 a5081160 791f2f30 152c11a5 11b65b53  
 5b4f791b 79131160 00000000 89718165  
 11603a00 1d95791b 00000000 89711123  
 4155791b 4944837a 11200000 000d0061  
 a5081160 1136837c 11295b42 00810061  
 491b7944 110e0000 79031160 188c7e61  
 2f3a7917 30001196 49421192 65000000  
 7d 9df7004e

9d

872a5b1b 5b53793b 5b4a7933 792b1160  
 793f1160 a5081160 a5081160 817d1100  
 49175b17 5b5a7937 4947794a 0827616f  
 4144793f 11603a00 2f3a792f bab26f61  
 a5081160 41567937 11605b5d 2a22617e  
 5b52793b a5081160 792fa508 39ad7e61  
 11604955 794b2f3a 1160493f 29b87e61  
 79172f30 79331160 41555b4c 34287e7e  
 9d 30d73ee9

Figure 9, Continued



7e  
dfcd7849 495e8d8d 79344942 55047850  
f706872e 8372791b 792c4943 48401783  
79121160 49308b72 837e112e 551b8ae0  
48551780 83707917 81651133 819a1106  
7949f726 49228b70 838d000c 8376112a  
f1c24955 838d8567 553816f0 838e1120  
794bf726 79304940 c1388b8d 817e1112  
f1c1a710 79334941 c11b82e0 858d5557  
7e 9b41445c

8d  
014c141c 014c1424 53250580 014e5416  
014c541c 014c5424 53d4b400 014e941c  
53d45468 0149d400 86000000 014e7400  
86cccccc 86cccccc 9b68a3d7 8e800000  
8abae147 00000000 768f5c28 8e000000  
82000000 00000014 6e3be8d3 58090000  
00000000 00010000 00000000 00010000  
00000000 00000000 00000000 5b000000  
8d f5417265

8e  
817c7933 11b4818d 897e8168 112d0000  
4918897e 55181600 837e1129 1b008168  
00008176 c118113e 817c7927 838e112a  
792f491a 80e0553b 4905897e 818e1194  
89768170 78504820 81702800 838e11a1  
1106838d 17315537 49028970 8172118e  
28004938 88e0792b 818f1100 00060000  
8b8d838c 817c4905 c137898d 00000000  
8e ef76a51c

8f  
8372791b c15ac15c 7952492f 494b8d63  
49308b72 555e16f0 8b6e838f 85600000  
83767917 c15e8d8d 11aa816b 83911120  
493a8b76 0006836e 552d7852 856411e9  
837c791f 794c4920 480617ae 495711b2  
49388b7c 79504921 856c7933 838c11b4  
858d5558 79554922 49468d6c 872f793a  
179c1701 79534923 8563792f 00008172  
8f f3feb43c

Figure 9, Continued

91

793f495c 0000856c 898c858d 1bac793b  
 8d60858c 792f4946 81905559 f701792l  
 793b494c 8d6c8163 c11f84e0 790e872f  
 839211b4 792b490b 2800495a 49577953  
 858c7933 89638160 7917495b 839111a1  
 494c8d8c 7927491c 7904495c 00000000  
 795b8564 8960818c 7909495d 83911130  
 838c1130 7923490c 83921120 00001191  
 91 132db311

92

7907495e 1160495f 553780df c11b5519  
 5b05113c 1128815e 552c7820 898d112c  
 551f8ce0 79374902 486017a6 855e793b  
 1606858d 895e8542 83931120 49428d5e  
 c1598d8d 818d551b 55198ce0 839311a7  
 1ba58d8c c13780e0 551a17ba 83981b35  
 836c11a5 552c7820 112bcella 8150570f  
 4115793f 485017b9 551b16f0 00a1007e  
 92 0f4a195

93

818d872a 11604952 17b50000 00000000  
 410c5b0a 553c4050 83541120 0000c11a  
 793f1160 5b16793b 818d553c 83941131  
 4953410c a5081160 872a5a60 00000000  
 790a2f3a 485017a5 41167937 00000000  
 793fa508 553c4060 a5081160 3abd7e6f  
 11604153 5b167937 486017ae 31a16f7e  
 3a02793b 11604860 83921132 b82c6161  
 93 3188871f

94

2936c137 16001fa5 839611ba 55357820  
 84df5535 11a01b29 551c1630 486017a3  
 872f7926 8397112c c11ac11c 818d113f  
 40601160 58005b00 898dcl3b 81591100  
 df80df80 551e1726 858280e0 8394113c  
 17a8791f 1606160a 55357820 8393112a  
 f701791d c11e551c 485017b6 8194110c  
 4d215537 c11a898d 553b80df 83951b20  
 94 e9f0b72f

Figure 9, Continued

95  
 790c4956 40605b16 818d551e 41165b18  
 818b793f 793ba508 17a6172e 792fa508  
 4916898b 11604860 83981122 83961120  
 818d552f 17218180 8d828182 a0026100  
 872a5b16 1180818d 8567553e 00000000  
 4050793b 551c8cdf 78204850 872f5500  
 11604850 818b7937 17360000 a9b86f6f  
 1730552f 4916898b 0006872a 839511b1  
 95 1a115a5e

96  
 11604945 11604946 4918897c c119898d  
 414f5b57 1131551e 83981120 83991120  
 793f1160 17a9c11e 78504860 00000000  
 49494116 553611be 172a551c 83971120  
 79182f3a 817c7937 8cded1600 00008172  
 793fa508 4918897c 1601c11d 8396113d  
 11605b45 83971139 898d13a5 aad16f7e  
 3006793b 817c7933 112fc11b b82c616f  
 96 f386919b

97  
 551d1724 8163793f c5394149 85640000  
 c11d0000 490b3963 7933a508 838c1130  
 83941120 818c793b 1160872a 00000000  
 551d160a 490c898c 5b39792f 00b2007e  
 c11d398d 791b817f 11604940 aa220102  
 791ff701 11230000 00000000 00000000  
 839611a5 87124149 00000000 839111a1  
 839611a5 79331160 81771100 856411c9  
 97 4a7832c7

98  
 00000000 791b4943 551c160a 81587933  
 00000000 8d4f818d c11d898d 491f8958  
 818d553b 791d4947 839611ba 113e0000  
 8396112a 81988341 5b5b7937 81591100  
 8542790c 81401185 2f30793b 835eb339  
 4940790d 8158792f a5081160 77333333  
 49417911 491f8958 1d230000 3a066100  
 4942816e 8393112a 83541120 00000000  
 98 321798d1

Figure 9, Continued



99  
 15341138 dfe81124 2422bb02 2428e830  
 872e793f 243a7df8 04452eel 0473e6d2  
 1160816e 04ccced1 04f2134a 05128f66  
 490f896e 05475155 055e9ca2 056f1798  
 793ff701 058cfad4 0598f354 05a33fel  
 83971121 05b39lef 05b9e57f 05bf29b2  
 dfc9dfda 05c6el40 05e97892 05eb499a  
 dfc5df80 05ecb84b 05ec24ca 5b0000a8  
 99 cl2f6cl7

9a  
 4953797f 4add1142 a7104d5d 8b8d837e  
 51577950 04000258 838d7938 79134925  
 1f797977 79511f51 a5106735 8b7e0000  
 495d795f 614f4dd1 19121116 81681129  
 00000000 38006d5d 8172119c 838e112a  
 79451160 3a007953 5538cl3d 00000006  
 695d4977 859911eb 16f0cl38 28006de7  
 6add616f 00030083 00000000 119a0054  
 9a 1d254bd5

Figure 9, Concluded

Constant Area Nozzle Program

The program is started by typing 7300.

1. Input Data. The input data consists of the following:  $k_e$ ,  $M_e$ , and  $N''$  where  $N''$  is the number of points on the leading Mach line to be calculated.
2. Output Data. The output consists of  $x$ ,  $y$ ,  $M^*$ ,  $M$ ,  $\theta$ , and  $\alpha$  for each point along the leading characteristic line.



## COMPUTER PROGRAM

```

73
85747911 795b701 795e1160 a5081160
f701555f 171e7911 3a004153 3a004153
7843f706 f7017940 795ea508 79561160
872e795f 4946872a 116030b0 30005b48
11604843 5b46302d 5b48795a 7956a508
17087911 795fa508 11604944 11603000
f701555b 11604948 41417957 5b577952
7849f706 41415b57 2f3a795a 83751160
73 18e833b5

```

```

74
53150f80 53050f80 531d0000 53bd0000
53e50000 53176000 45400000 6683d994
53151a00 00000000 b22a0102 00000000
00000000 00000000 6e3be8d3 39257e61
00000000 5196724a a8207e61 8a00000c
00000000 9400616f 970f6f7e 86000000
00000000 0e376f7e 0796616f 58060000
00020061 ab237e61 8e067e61 99036f90
74 bf04da0b

```

```

75
30005b44 794f1160 e54b8712 30005b46
7952a508 87293000 794e1160 795da508
11608729 79111160 c554414b 11604958
3000790e 872a3022 794ea508 5b4b414e
11604945 5b57794f 1160e550 79591160
794d4947 a5081160 872a4142 49484150
872a4148 8713300d 79572f3a 5b497955
79572f3a 792a1160 795a1160 81761160
75 351480e6

```

```

76
49434154 1b00555b 494911b7 8371791f
5b497959 872f7939 553b790f 4927db71
a5081160 40491160 f701784a 81651b00
2f305b57 795b701 f706793f 00000000
7955a508 17057904 f70117ea 00000000
11604944 f701872a 791ef701 00000000
00001181 41495b58 41405b40 00060000
7951f706 795e1160 791f1109 58000000
76 fe5e78f0

```

Figure 10

Tape Program

This program puts the last right running characteristic line on punched tape. The program can then be used to transfer the points to their proper locations for the Newtonian boundary program. To put the points on tape, type 9b01. To transfer the points into the Newtonian boundary program, type 9b00.

1. Input data. The number of points is stored in channel 9b, word 17 in the following form:

00 (N) 0000

where N represents the number of points.

## COMPUTER PROGRAM

9b  
872a1110 00007917 11604840 00000000  
79174a08 4d09551f 17985517 00000000  
16001f9e 16001f99 8af0178e 6e3be8d3  
c11fc117 c11f82e0 1b000000 0082006f  
551bf108 551b7840 00000000 00020000  
48401790 f5081791 00000000 00050000  
55134040 11851b01 00000000 00060000  
111d1b00 5b0b790f 00000000 00000000  
9b f37ed55e

Figure 11